

Form factors of $B_{(s)}$ to light scalar mesons with the B -meson light-cone sum rules

R. Khosravi*

Department of Physics, School of Science, Shiraz University, Shiraz 71946-84795, Iran (Received 7 August 2023; accepted 5 January 2024; published 5 February 2024)

In this work, the transition form factors of the semileptonic decays of $B_{(s)}$ to the light scalar mesons with masses close to 1.5 GeV such as $K_0^*(1430)$, $a_0(1450)$, and $f_0(1500)$ are calculated in the framework of the light-cone sum rules. For this purpose, the two- and three-particle B -meson distribution amplitudes (DAs) are used. Note that it is possible to use the B -meson DAs for the B_s meson in the $SU(3)_F$ symmetry limit. The transition form factors are obtained in terms of the two-particle DAs up to twist-five accuracy, and the three-particle up to twist-six level. We apply two classes of the phenomenological models for the DAs of the B meson. The longitudinal lepton polarization asymmetries and branching fractions for the semileptonic decays of $B_{(s)}$ to the light scalar mesons are estimated with the help of these form factors.

DOI: [10.1103/PhysRevD.109.036003](https://doi.org/10.1103/PhysRevD.109.036003)

I. INTRODUCTION

Although scalar states with $J^P = 0^+$ have been observed for more than half a century, their inner structure is still controversial both experimentally and theoretically. In order to discover their underlying structure, many different theoretical and phenomenological descriptions are presented including considering the scalar mesons as the conventional mesons $q\bar{q}$ or nonconventional mesons such as tetraquark [1], molecule [2], hybrid [3], and glueballs [4]. A tetraquark is a complex structure made up of one diquark and one antidiquark $qq - \bar{q}\bar{q}$. A molecule or a meson-meson bound state is composed of two quark-antiquark couples $q\bar{q} - q\bar{q}$. In addition, a hybrid is an object consisting of a $q\bar{q}$ pair with at least one extra gluon $q\bar{q} - g$, and the glueballs are made only of gluons (for instance see Ref. [5]). It is very likely that some scalar mesons are not made of one simple component but are the superpositions of these contents. For example, it is suggested that $a_0(980)$ is a superposition of $q\bar{q}$ and tetraquark [6]. The dominant component of the scalar mesons can be found from the decay and production of them.

A number of the scalar mesons have been discovered in the spectroscopic studies. Because of the large decay widths of the scalar mesons, the identification of them is more difficult in contrast to the pseudoscalars and vector mesons. Among them, there are nine light scalar mesons together, below or near 1 GeV, including the isoscalars

$f_0(500)$ (also denoted as σ) and $f_0(980)$, isodoublets [$K_0^{*+}(700)$ (also referred as κ), $K_0^{*0}(700)$] and [$\bar{K}_0^{*0}(700)$, $\bar{K}_0^{*-}(700)$], and isovector [$a_0^+(980)$, $a_0^0(980)$, $a_0^-(980)$] which can form an $SU(3)$ nonet, while the scalar mesons around 1.5 GeV, consisting of isoscalars $f_0(1370)$ and $f_0(1500)/f_0(1700)$, isodoublets [$K_0^{*+}(1430)$, $K_0^{*0}(1430)$] and [$\bar{K}_0^{*0}(1430)$, $\bar{K}_0^{*-}(1430)$], and isovector [$a_0^+(1450)$, $a_0^0(1450)$, $a_0^-(1450)$] can be members of another nonet. From a survey of the accumulated experimental data, two scenarios can be suggested to describe these two groups of nine scalar mesons in the quark model [7]. In the first one, scenario 1 (S1), it is supposed that the light scalar mesons are composed from two quarks. The nonet mesons below 1 GeV are treated as the lowest lying states, and the nonet mesons near 1.5 GeV are the excited states corresponding to the lowest lying states. In scenario 2 (S2), the scalar states below 1 GeV are considered as the members of a tetraquark nonet, while the nonet mesons near 1.5 GeV are viewed as the lowest lying states, with the corresponding first excited states between 2.0–2.3 GeV. In both scenarios, it is suggested that the heavier nonet near 1.5 GeV consists of the scalar mesons with two quarks in the quark model. However in S1, those are regarded as the excited states, and in S2 they are seen as the ground states. Therefore, the calculation of the decay constant values and DAs for the scalar mesons near 1.5 GeV are different via the two scenarios.

In recent years, some experimental efforts have been devoted to measuring the decay modes involving the light scalar mesons in final state. The BESIII Collaboration has recently measured the nonleptonic and semileptonic decays of D_s to the light scalar mesons [8–10]. In the same context, the nonleptonic two-body B -meson decays

*rezakhosravi@saadi.shirazu.ac.ir

Published by the American Physical Society under the terms of the [Creative Commons Attribution 4.0 International license](https://creativecommons.org/licenses/by/4.0/). Further distribution of this work must maintain attribution to the author(s) and the published article's title, journal citation, and DOI. Funded by SCOAP³.

involving a scalar final state have been observed by Belle [11], *BABAR* [12], and LHCb [13]. These observations provide an efficient way to investigate the features and the possible inner structures of the scalar mesons.

In the particle physics an accurate calculation of the transition form factors for the semileptonic $B_{(s)}$ decays to the light scalar mesons is important in two folds. First, to study the quantities related to the semileptonic and non-leptonic decays involving $B_{(s)}$ to the scalar mesons, it is necessary to know the appropriate behavior of the transition form factors. Second, for the indirect search of new physics beyond the standard model (SM), these form factors are the essential ingredients. Since the heavy to light transition form factors are nonperturbative in nature, the nonperturbative QCD approaches are applied to evaluate them. Usually, the lattice QCD (LQCD) works well to calculate the form factors in these cases.

So far, the transition form factors of $B_{(s)} \rightarrow S$, [$S = K_0^*(1430), a_0(1450), f_0(1500)$] have been not estimated through the LQCD, although they have been calculated from other methods such as the perturbative QCD (pQCD) [14], covariant light front (CLF) [15], QCD sum rules (QCDSR) [16–18], light-front quark model (LFQM) [19], minimal supersymmetric standard model (MSSM) [20], and also the light-cone sum rules (LCSR).

The LCSR is a proper approach to evaluate the transition form factors of the heavy to light meson decays. The conventional LCSR starts with a two-point correlation function inserting the operators between vacuum and light meson. Then, it develops in terms of the nonlocal operators by using the operator product expansion (OPE) near the light-cone region $x^2 = 0$. The matrix elements of the nonlocal operators are parametrized as the light meson DAs of the increasing twist, i.e., twist-two, twist-three, twist-four, and so on. These DAs offer valuable insights into the nonperturbative makeup of hadrons and the distribution of partons in relation to their momentum fractions within these particles. More research on the $B_{(s)} \rightarrow S$ transition form factors have been performed in the framework of the LCSR with the light scalar meson twist-two and twist-three DAs [21–23], only scalar meson twist-two DA [24,25], or twist-three DAs [26], respectively. In this method, a reliable estimation of the form factors depends on an accurate knowledge of the internal structure of the light meson and its DAs. Since the intrinsic nature of the light scalar mesons is still not completely clear, the DAs attributed to them can also be doubted. Therefore, it is important to use a new LCSR method to calculate the form factors that is independent of the light scalar meson DAs, and then compare its results with the conventional method.

In Ref. [27], the authors proposed a new method based on the LCSR technique that relates the B -meson DAs to the $B \rightarrow \pi$ form factor. This model was independently suggested in the framework of the soft-collinear effective theory (SCET) in Ref. [28]. In this new approach, which

is sometimes called the B -meson LCSR, the main idea is to invert the correlation function compared to the conventional LCSR, so that the light meson interpolates with an appropriate light-quark current, and the nonlocal operators between an on-shell B -meson state and the hadronic vacuum are expressed as convolutions of hard scattering kernels with light-cone distribution amplitudes (LCDAs) of the B meson. Recently, considering the next-to-leading order QCD corrections to the correlation function in order to extract the hard and jet functions, the form factors of semileptonic decays B to scalar mesons have been calculated in terms of leading twist function of the B -meson DA [29]. Also, considering the $SU(3)_F$ symmetry limit and using the two-particle B -meson DAs up to twist-three, and three-particle DAs up to twist-four, the transition form factors of the semileptonic $B_s \rightarrow K_0^*(1430)$ decays have been calculated in the framework of the B -meson LCSR [30].

In this work, we focus on the three light scalar mesons $K_0^*(1430), a_0(1450),$ and $f_0(1500)$, with the mass of about 1.5 GeV. The production of the light scalar mesons $K_0^*, a_0,$ and f_0 can provide a different unique insight to the mysterious structure of them. Our main goal is to calculate the form factors of the $B_{(s)} \rightarrow (K_0^*, a_0, f_0)$ decays via the B -meson LCSR applying the two-particle DAs up to twist-five, and considering the new results for the complete set of the three-particle DAs up to twist-six. The four-particle B -meson DAs are not taken into account in this work due to the negligible effects. Note that in the $SU(3)_F$ symmetry limit, it is possible to use the B -meson DAs for the B_s meson. The functional form of the higher-twist B -meson DAs involve contributions of multiparton states. To calculate the form factors, we use two classes of the phenomenological models for the two- and three-particle DAs of the B meson which contain a minimum number of free parameters and satisfy equation of motion (EOM) constraints in tree level [31,32]. Utilizing these form factors, the semileptonic $B_{(s)} \rightarrow (K_0^*, a_0)l\bar{\nu}_l$ and $B_{(s)} \rightarrow (K_0^*, f_0)\bar{l}l/\nu\bar{\nu}$, $l = e, \mu, \tau$ decays are analyzed. In the SM, the rare semileptonic $B_{(s)} \rightarrow (K_0^*, f_0)\bar{l}l/\nu\bar{\nu}$ decays occur at loop level instead of tree level, by electroweak penguin and weak box diagrams via the flavor changing neutral current (FCNC) transitions of $b \rightarrow sl^+l^-$ at quark level.

The content of paper is as follows: In Sec. II, the form factors of the semileptonic $B_{(s)} \rightarrow S$, ($S = K_0^*, a_0, f_0$) decays are calculated with the B -meson LCSR approach using the two- and three-particle DAs of the B meson up to twist-five, and twist-six, respectively. These form factors are basic parameters to study the other quantities such as forward-backward asymmetry, longitudinal lepton polarization asymmetry, and the branching fraction of semileptonic decays. In Sec. III, the two phenomenological models for the DAs of the B meson are presented.

This section is also devoted to the numerical and analytical results for the semileptonic $B_{(S)} \rightarrow S$ decays.

II. FORM FACTORS OF $B_{(S)} \rightarrow S$ WITH HIGHER-TWIST CORRECTIONS

Considering parity and using Lorentz invariance, the transition matrix elements involved in $B_{(S)} \rightarrow S$ transitions can be parametrized as

$$\begin{aligned} \langle S(p') | J_\mu^A | B_{(S)}(p) \rangle &= -i [f_+(q^2) P_\mu + f_-(q^2) q_\mu], \\ \langle S(p') | J_\mu^T | B_{(S)}(p) \rangle &= -\frac{f_T(q^2)}{m_{B_{(S)}} + m_S} [q^2 P_\mu - (m_{B_{(S)}}^2 - m_S^2) q_\mu]. \end{aligned} \quad (1)$$

In these phrases $P_\mu = (p' + p)_\mu$, $q_\mu = (p - p')_\mu$. The transition currents $J_\mu^A = \bar{q}_1 \gamma_\mu \gamma_5 b$, and $J_\mu^T = \bar{q}_1 \sigma_{\mu\nu} \gamma_5 q^\nu b$ ($q_1 = u, s$) are used to calculate the transition form factors $f_+(q^2)$, $f_-(q^2)$ and $f_T(q^2)$, respectively. q^2 is the momentum transfer squared. The calculation of these form factors using the LCSR method is described in this section.

To investigate the form factors in the frame work of the B -meson LCSR, the two-point correlation function $\Pi(p', q)$ is constructed from two currents inserted between vacuum and $B_{(S)}$ meson as follows:

$$\Pi(p', q) = i \int d^4x e^{ip' \cdot x} \langle 0 | T \{ J^S(x) J(0) \} | B_{(S)}(p) \rangle, \quad (2)$$

where T is the time ordering operator, and $J^S(x)$ is the interpolating current of the scalar meson S , so that $J^{K_0^{*+}}(x) = \bar{s}(x)u(x)$, $J^{K_0^{*0}}(x) = \bar{d}(x)s(x)$, $J^{a_0}(x) = \bar{d}(x)u(x)$, and $J^{f_0}(x) = \bar{s}(x)s(x)$. The matrix element of J^S between the vacuum and scalar meson S is given in terms of the decay constant f_S , and mass of the scalar meson as $\langle 0 | J^S | S \rangle = f_S m_S$. In the correlation function, $J(0)$ is the transition current; $J = J_\mu^A$ or J_μ^T . In addition, p' and q are the momenta of the interpolating and transition currents, respectively. The relation between these two quantities is $p^2 = (p' + q)^2 = m_{B_{(S)}}^2$.

The correlation function in Eq. (2) can be investigated from two aspects, hadronic representation and QCD calculations. The form factors are obtained via the LCSR method in terms of the DAs of the B meson by equating the two sides. As mentioned before, it is possible to use the B -meson DAs for B_s -meson in the $SU(3)_F$ symmetry limit.

A. Hadronic representation

Inserting a complete set of the intermediate states with the same quantum number as the interpolating current J^S , in Eq. (2), and isolating the pole term of the lowest scalar meson S , and then applying the Fourier transformation, the hadronic representation of the correlation

function is obtained. Defining the spectral density function of the higher resonances and continuum states as $\rho(s) \equiv \sum_h \langle 0 | J^S(p') | h(p') \rangle \langle h(p') | J | B_{(S)}(p) \rangle \delta(s - m_h^2)$, the correlation function can be written in terms of the scalar meson state and the higher resonance contributions as

$$\begin{aligned} \Pi^{\text{HAD}}(p', q) &= \frac{\langle 0 | J^S | S(p') \rangle \langle S(p') | J | B_{(S)}(p) \rangle}{m_S^2 - p'^2} \\ &+ \int_{s_0}^{\infty} ds \frac{\rho(s)}{s - p'^2}, \end{aligned} \quad (3)$$

where s_0 is the continuum threshold of the scalar meson S .

B. QCD calculations

At the quark level in QCD, the correlation function can be evaluated in the deep Euclidean region as a complex function. Using the dispersion relation, the correlation function can be written as

$$\Pi^{\text{QCD}}(p', q) = \frac{1}{\pi} \int_0^{\infty} ds \frac{\text{Im} \Pi^{\text{QCD}}(s)}{s - p'^2}. \quad (4)$$

Applying the Borel transformation in Eqs. (3) and (4) with respect to the variable p'^2 as $\mathbf{B}_{p'^2}(\frac{1}{x^2 - p'^2}) = \frac{e^{-x^2/M^2}}{M^2}$, where M^2 is the Borel parameter, guarantees that the contributions of the higher states and continuum in the hadronic representation are effectively suppressed. In addition, it assures that the contributions of higher-dimensional operators in the QCD side are small. Equating both sides of the correlation function, and using the quark-hadron duality approximation at large spacelike p'^2 as $\rho(s) \simeq \frac{1}{\pi} \text{Im} \Pi^{\text{QCD}}(s)$, the following equality is determined:

$$\langle 0 | J^S | S(p') \rangle \langle S(p') | J | B_{(S)}(p) \rangle e^{-m_S^2/M^2} = \int_0^{s_0} ds \rho(s) e^{-s/M^2}. \quad (5)$$

Investigating the spectral density at the quark level allows us to derive the form factors f_+ , f_- and f_T in Eq. (5).

Based on the heavy quark effective theory (HQET), the $B_{(S)}$ -meson state in the limit of large m_b can be estimated by the relativistic normalization of it $|B_{(S)}(p)\rangle = |B_{(S)}(v)\rangle$, where v is four-velocity of the $B_{(S)}$ meson. Up to $1/m_b$ corrections, the correlation function of the $B_{(S)} \rightarrow S$ transition can be approximated as $\Pi^{\text{QCD}}(p', q) = \tilde{\Pi}^{\text{QCD}}(p', \tilde{q}) + \mathcal{O}(1/m_b)$, where $\tilde{q} = q - m_b v$ is called the static part of q . Replacing the b -quark field by the HQET field h_v , the correlation function [Eq. (2)] in the heavy quark limit, ($m_b \rightarrow \infty$), becomes [33]

$$\tilde{\Pi}^{\text{QCD}}(p', \tilde{q}) = i \int d^4x e^{ip' \cdot x} \langle 0 | T \{ \bar{q}(x) S_{q_1}(x) \Gamma h_v(0) \} | B(v) \rangle, \quad (6)$$

where quark field \bar{q} stands for \bar{s} or \bar{d} , and a matrix composition Γ is $\gamma_\mu\gamma_5$ or $\sigma_{\mu\nu}\gamma_5 q^\nu$ corresponding to the transition currents J_μ^A or J_μ^T , respectively. The full-quark propagator $S_{q_1}(x)$ of a massless quark q_1 (u or s) in the external gluon field in the Fock-Schwinger gauge is as follows [34]:

$$S_{q_1}(x) = i \int \frac{d^4k}{(2\pi)^4} e^{-ik \cdot x} \left\{ \frac{k}{k^2} + \int_0^1 du G_{\lambda\rho}(ux) \left[\frac{1}{k^2} u x^\lambda \gamma^\rho - \frac{1}{2k^4} k \sigma^{\lambda\rho} \right] \right\}. \quad (7)$$

If the full-quark propagator $S_{q_1}(x)$ in Eq. (7) is replaced in Eq. (6), operators between vacuum mode and $B(v)$ state create the nonzero matrix elements as $\langle 0 | \bar{q}_{\alpha(x)h_{v\beta}(0)} | B(v) \rangle$ and $\langle 0 | \bar{q}_\alpha(x) G_{\lambda\rho}(ux) h_{v\beta}(0) | B(v) \rangle$. These matrix elements of the nonlocal heavy-light currents are parametrized in terms of the B -meson DAs. The two-particle higher-twist DAs of the B meson arise in the expansion of the relevant nonlocal quark-antiquark operator close to the light cone as [31,32,35]

$$\langle 0 | \bar{q}_{\alpha(x)h_{v\beta}(0)} | B(v) \rangle = -\frac{if_B m_B}{4} \int_0^\infty d\omega e^{-i\omega v \cdot x} \left\{ (1 + \not{v}) \left[(\varphi_+(\omega) + x^2 g_+(\omega)) - \frac{\not{x}}{2v \cdot x} [(\varphi_+(\omega) - \varphi_-(\omega)) + x^2 (g_+(\omega) - g_-(\omega))] \right] \gamma_5 \right\}_{\beta\alpha}, \quad (8)$$

where $\varphi_+(\omega)$, $\varphi_-(\omega)$, $g_+(\omega)$, and $g_-(\omega)$ are of leading twist, twist-three, twist-four, and twist-five, respectively. The three-particle contributions involve a further gluon field, so that the matrix elements of the nonlocal operator $q_\alpha(x) G_{\lambda\rho}(ux) h_{v\beta}(0)$ are parametrized in terms of the B -meson DAs of increasing twist as [31,32,35]

$$\begin{aligned} \langle 0 | \bar{q}_\alpha(x) G_{\lambda\rho}(ux) h_{v\beta}(0) | B(v) \rangle = & \frac{f_B m_B}{4} \int_0^\infty d\omega \int_0^\infty d\xi e^{-i(\omega+u\xi)v \cdot x} \left\{ (1 + \not{v}) \left[(v_\lambda \gamma_\rho - v_\rho \gamma_\lambda) (\Psi_A(\omega, \xi) - \Psi_V(\omega, \xi)) \right. \right. \\ & - i \sigma_{\lambda\rho} \Psi_V(\omega, \xi) - \frac{x_\lambda v_\rho - x_\rho v_\lambda}{v \cdot x} X_A(\omega, \xi) + \frac{x_\lambda \gamma_\rho - x_\rho \gamma_\lambda}{v \cdot x} (W(\omega, \xi) + Y_A(\omega, \xi)) \\ & - i \epsilon_{\lambda\rho\delta\eta} \frac{x^\delta v^\eta \gamma_5}{v \cdot x} \bar{X}_A(\omega, \xi) + i \epsilon_{\lambda\rho\delta\eta} \frac{x^\delta \gamma^\eta \gamma_5}{v \cdot x} \bar{Y}_A(\omega, \xi) - u \frac{x_\lambda v_\rho - x_\rho v_\lambda}{(v \cdot x)^2} \not{x} W(\omega, \xi) \\ & \left. \left. + u \frac{x_\lambda \gamma_\rho - x_\rho \gamma_\lambda}{(v \cdot x)^2} \not{x} Z(\omega, \xi) \right] \gamma_5 \right\}_{\beta\alpha}. \quad (9) \end{aligned}$$

There exist eight independent Lorentz structures and therefore eight invariant functions; Ψ_A , Ψ_V , X_A , Y_A , \bar{X}_A , \bar{Y}_A , W , and Z are the eight independent three-particle DAs of the B meson. The three-particle DAs are related to a basis of DAs such as ϕ_i ($i = 3, \dots, 6$), ψ_j and $\bar{\psi}_j$ ($j = 4, 5$) with definite twist (i and j indicate the twist level) as follows:

$$\begin{aligned} \Psi_A(\omega, \xi) &= \frac{1}{2} [\phi_3 + \phi_4], & \Psi_V(\omega, \xi) &= \frac{1}{2} [-\phi_3 + \phi_4], \\ X_A(\omega, \xi) &= \frac{1}{2} [-\phi_3 - \phi_4 + 2\psi_4], & Y_A(\omega, \xi) &= \frac{1}{2} [-\phi_3 - \phi_4 + \psi_4 - \psi_5], \\ \bar{X}_A(\omega, \xi) &= \frac{1}{2} [-\phi_3 + \phi_4 - 2\bar{\psi}_4], & \bar{Y}_A(\omega, \xi) &= \frac{1}{2} [-\phi_3 + \phi_4 - \bar{\psi}_4 + \bar{\psi}_5], \\ W(\omega, \xi) &= \frac{1}{2} [\phi_3 - \psi_4 - \bar{\psi}_4 + \phi_5 + \psi_5 + \bar{\psi}_5], & Z(\omega, \xi) &= \frac{1}{4} [-\phi_3 + \phi_4 - 2\bar{\psi}_4 + \phi_5 + 2\bar{\psi}_5 - \phi_6]. \quad (10) \end{aligned}$$

Substituting the appropriate expressions of Eqs. (8) and (9) instead of the matrix elements $\langle 0 | \bar{q}_{1\alpha(x)h_{v\beta}(0)} | B(v) \rangle$ and $\langle 0 | \bar{q}_{1\alpha}(x) G_{\lambda\rho}(ux) h_{v\beta}(0) | B(v) \rangle$ that appear in the correlation function in Eq. (6), and integrating over the variables x and k , and then separating the solutions according to the Lorentz structures P_μ and q_μ , the general form of the correlation function, $\tilde{\Pi}^{\text{QCD}}(p', \bar{q})$ can be written as $i[\tilde{\Pi}_+^A(p', \bar{q})P_\mu + \tilde{\Pi}_-^A(p', \bar{q})q_\mu]$ and $\tilde{\Pi}^T(p', \bar{q})P_\mu$ corresponding to J_μ^A and J_μ^T , respectively.

Finally, inserting Eq. (1) in Eq. (3), and then equating the coefficients of the same Lorentz structures on both sides of the correlation function, the form factors are obtained via the LCSR in terms of the two- and three-particle DAs of the B meson. Our results for $f_+(q^2)$, $f_-(q^2)$, and $f_T(q^2)$ are obtained as

$$\begin{aligned}
f_+(q^2) &= \frac{f_{B_{(s)}} m_{B_{(s)}}^2}{2f_S m_S} e^{\frac{m_S^2}{M^2}} \int_0^{\sigma_0} d\sigma e^{-\frac{s(\sigma)}{M^2}} \left\{ \varphi_+(\sigma m_{B_{(s)}}) - \frac{\tilde{\varphi}(\sigma m_{B_{(s)}})}{\bar{\sigma} m_{B_{(s)}}} - \frac{4g_+(\sigma m_{B_{(s)}})}{\bar{\sigma} M^2} \right. \\
&\quad + \int_0^{\sigma m_{B_{(s)}}} d\omega \int_{\sigma m_{B_{(s)}} - \omega}^{\infty} \frac{d\xi}{\xi} \left\{ \left[(2u+2) \left(\frac{\bar{q}^2}{\bar{\sigma}^3 M^2} + \frac{1}{\bar{\sigma}^2} \right) + \frac{(2u+1)m_{B_{(s)}}^2}{\bar{\sigma} M^2} \right] \frac{\tilde{\Psi}(\omega, \xi)}{m_{B_{(s)}}^2} \right. \\
&\quad + \frac{6u}{\bar{\sigma} M^2} \Psi_V(\omega, \xi) + \left[(2u-1) \left(\frac{\bar{q}^2}{\bar{\sigma}^3 M^4} + \frac{1}{\bar{\sigma}^2 M^2} \right) + \frac{3}{\bar{\sigma}^2 M^2} \right] \frac{\tilde{X}_A(\omega, \xi)}{m_{B_{(s)}}} - \frac{4(u+3)}{\bar{\sigma}^2 M^2} \frac{\tilde{Y}_A(\omega, \xi)}{m_{B_{(s)}}} \\
&\quad \left. \left. - \left(\frac{\bar{q}^2}{\bar{\sigma}^3 M^4} + \frac{1}{\bar{\sigma}^2} \right) \frac{\tilde{X}_A(\omega, \xi)}{m_{B_{(s)}}^2} - \frac{4u}{m_{B_{(s)}}^2} \left(\frac{\bar{q}^2}{\bar{\sigma}^4 M^4} - \frac{m_{B_{(s)}}^2}{\bar{\sigma}^2 M^4} - \frac{2}{\bar{\sigma}^2 M^2} \right) \tilde{W}(\omega, \xi) - \frac{48u}{\bar{\sigma}^2 M^4} \tilde{Z}(\omega, \xi) \right\} \right\}, \\
f_-(q^2) &= -\frac{f_{B_{(s)}} m_{B_{(s)}}^2}{2f_S m_S} e^{\frac{m_S^2}{M^2}} \int_0^{\sigma_0} d\sigma e^{-\frac{s(\sigma)}{M^2}} \left\{ \frac{(1+\sigma)}{\bar{\sigma}} \varphi_+(\sigma m_{B_{(s)}}) + \frac{\tilde{\varphi}(\sigma m_{B_{(s)}})}{\bar{\sigma} m_{B_{(s)}}} - \frac{4(1+\sigma)}{\bar{\sigma}^2 M^2} g_+(\sigma m_{B_{(s)}}) \right. \\
&\quad - \int_0^{\sigma m_{B_{(s)}}} d\omega \int_{\sigma m_{B_{(s)}} - \omega}^{\infty} \frac{d\xi}{\xi} \left\{ \left[(2u+2) \left(\frac{\bar{q}^2}{\bar{\sigma}^3 M^2} + \frac{1}{\bar{\sigma}^2} \right) - \frac{(2u+1)(1+\sigma)m_{B_{(s)}}^2}{\bar{\sigma}^2 M^2} \right] \frac{\tilde{\Psi}(\omega, \xi)}{m_{B_{(s)}}^2} \right. \\
&\quad + \frac{6u(1+\sigma)}{\bar{\sigma}^2 M^2} \Psi_V(\omega, \xi) + \left[\frac{(2u-1)(1+\sigma)}{\bar{\sigma}} \left(\frac{\bar{q}^2}{\bar{\sigma}^3 M^4} + \frac{1}{\bar{\sigma}^2 M^2} \right) + \frac{4(u+\bar{\sigma})}{\bar{\sigma}^3 M^2} \right] \frac{\tilde{X}_A(\omega, \xi)}{m_{B_{(s)}}} \\
&\quad - \frac{4(u+3)}{\bar{\sigma}^2 M^2} \frac{\tilde{Y}_A(\omega, \xi)}{m_{B_{(s)}}} - \left[\frac{(1+\sigma)(2q^2 - \bar{\sigma}^2)}{\bar{\sigma}^4 M^4} + \frac{3+\sigma}{\bar{\sigma}^3} \right] \frac{\tilde{X}_A(\omega, \xi)}{m_{B_{(s)}}^2} - \frac{48u(1+\sigma)}{\bar{\sigma}^3 M^4} \tilde{Z}(\omega, \xi) \\
&\quad \left. \left. + \frac{4u}{m_{B_{(s)}}^2} \left(\frac{\bar{q}^2}{\bar{\sigma}^4 M^4} + \frac{(1+\sigma)m_{B_{(s)}}^2}{\bar{\sigma}^3 M^4} - \frac{2}{\bar{\sigma}^2 M^2} \right) \tilde{W}(\omega, \xi) \right\} \right\}, \\
f_T(q^2) &= \frac{f_{B_{(s)}} m_{B_{(s)}}}{2f_S m_S} (m_{B_{(s)}} + m_S) e^{\frac{m_S^2}{M^2}} \int_0^{\sigma_0} d\sigma e^{-\frac{s(\sigma)}{M^2}} \left\{ \frac{\varphi_+(\sigma m_{B_{(s)}})}{\bar{\sigma}} + \int_0^{\sigma m_{B_{(s)}}} d\omega \int_{\sigma m_{B_{(s)}} - \omega}^{\infty} \frac{d\xi}{\xi} \left\{ \left[\frac{6u}{\bar{\sigma}^2 M^2} \right] \Psi_V(\omega, \xi) \right. \right. \\
&\quad + \left[\frac{2u+1}{\bar{\sigma}^2 M^2} \right] \tilde{\Psi}(\omega, \xi) - \left[\frac{\bar{q}^2}{\bar{\sigma}^4 M^4} + 2 \right] \frac{\tilde{X}_A}{m_{B_{(s)}}} - \left[\frac{\bar{q}^2}{2\bar{\sigma}^4 M^4} - \frac{1}{\bar{\sigma}^2 M^2} \right] \frac{\tilde{X}_A(\omega, \xi)}{m_{B_{(s)}}} - \frac{u\sigma m_{B_{(s)}}(1+\bar{\sigma})}{\bar{\sigma}^4 M^4} \tilde{W}(\omega, \xi) \\
&\quad \left. \left. - \frac{6u\sigma(1+\bar{\sigma})}{\bar{\sigma}^4 M^4} \tilde{Z}(\omega, \xi) \right\} \right\}, \tag{11}
\end{aligned}$$

where $\sigma = \omega/m_{B_{(s)}}$, $u = (\sigma m_{B_{(s)}} - \omega)/\xi$, $\mathbf{s}(\sigma) = \sigma m_{B_{(s)}}^2 - \frac{\sigma}{\bar{\sigma}} q^2$, $\bar{\sigma} = 1 - \sigma$, $\bar{\varphi} = \varphi_+ - \varphi_-$, $\tilde{\Psi} = \Psi_A - \Psi_V$,
 $\bar{q}^2 = q^2 - \bar{\sigma}^2 m_{B_{(s)}}^2$, $\sigma_0 = \frac{s_0 + m_{B_{(s)}}^2 - q^2 - \sqrt{(s_0 + m_{B_{(s)}}^2 - q^2)^2 - 4s_0 m_{B_{(s)}}^2}}{2m_{B_{(s)}}^2}$, and

$$\begin{aligned}
\tilde{\varphi}_{\pm}(\sigma m_{B_{(s)}}) &= \int_0^{\sigma m_{B_{(s)}}} d\tau \varphi_{\pm}(\tau), & \tilde{Y}_A(\omega, \xi) &= \int_0^{\omega} d\tau Y_A(\tau, \xi), \\
\tilde{X}_A(\omega, \xi) &= \int_0^{\omega} d\tau X_A(\tau, \xi), & \tilde{\tilde{X}}_A(\omega, \xi) &= \int_0^{\omega} d\tau \tilde{X}_A(\tau, \xi), \\
\tilde{W}(\omega, \xi) &= \int_0^{\xi} d\zeta \int_0^{\omega} d\tau W(\tau, \zeta), & \tilde{\tilde{Z}}(\omega, \xi) &= \int_0^{\xi} d\zeta \int_0^{\omega} d\tau Z(\tau, \zeta). \tag{12}
\end{aligned}$$

III. NUMERICAL ANALYSIS

This section encompasses our numerical analysis of the form factors f_+ , f_- , and f_T of the semileptonic decays $B_{(s)} \rightarrow S$, ($S = K_0^*(1430), a_0(1450), f_0(1500)$), branching fractions, longitudinal lepton polarization asymmetries, and discussion. The B -meson LCSR expressions of the form factors in Eq. (11) depict that the main input values are the masses

TABLE I. Masses and leptonic decay constants of mesons in GeV [7,36,37].

Meson	B	B_s	$K_0^*(1430)$	$a_0(1450)$	$f_0(1500)$
Mass	5.28	5.37	1.43 ± 0.05	1.47 ± 0.02	1.50 ± 0.00
Decay constant	0.19	0.23	0.45 ± 0.05	0.46 ± 0.05	0.49 ± 0.05

and leptonic decay constants of mesons. In addition, the two- and three-particle DAs of B -meson are the effective terms that must be specified in calculations of the form factors. The expressions of the form factors contain also two auxiliary parameters; Borel mass square M^2 and the continuum threshold s_0 of the scalar mesons.

The values for the masses and leptonic decay constants of B , B_s , $K_0^*(1430)$, $a_0(1450)$, and $f_0(1500)$ are given in Table I.

To continue, we need to specify appropriate functions for the DAs of the B meson. The B -meson light-cone DAs are the main nonperturbative input to the QCD description of weak decays involving light hadrons in the framework of QCD factorization. The knowledge about the behavior of the higher-twist B -meson DAs is still rather limited due to infrared divergences which appear in power-suppressed contributions. To overcome the divergences in these cases, some efforts have been made, including the calculation of nonperturbative contributions of B -meson decays in terms of increasing twist based on the LCSR approach [33,38–41]. One of the problems of this way is that the higher-twist B -meson DAs involve contributions of multiparton states and are practically unknown.

In Ref. [31], the authors present a systematic study of the higher-twist DAs of the B meson which give rise to power-suppressed $1/m_B$ contributions to B decays in final

states with energetic light particles in the framework of QCD factorization. As the main result, they find that the renormalization group equations for the three-particle distributions are completely integrable in the large N_c limit and can be solved exactly. Finally, they study the general properties of the solutions and suggest two simple models including the exponential (Exp) model, and local duality (LD) model for the higher-twist DAs of the B meson with a minimum number of free parameters which satisfy all tree-level EOM constraints and can be used in phenomenological studies. The authors in Ref. [32] construct the LD model for the twist-five and twist-six B -meson DAs, in agreement with the corresponding asymptotic behaviors at small quark and gluon momenta.

The Exp model is the simplest model based on combining the regime of low momentum of quarks and gluons with an exponential suppression at large momentum, whereas the LD model is based on the duality assumption to match the B -meson state with the perturbative spectral density integrated over the duality region. In this work, we apply these two models, Exp and LD models, for an estimation of the semileptonic form factors of $B_{(s)}$ to the light scalar mesons $K_0^*(1430)$, $a_0(1450)$, and $f_0(1500)$ via the B -meson LCSR. Note that in the $SU(3)_F$ symmetry limit, it is possible to use the B -meson DAs for the B_s meson.

A. Exp model

Combining the known low momentum behavior with an exponential fall-off at large quark and gluon momenta, and considering the normalization conditions, the Exp model can be obtained [31]. The shapes of the two-particle DAs $\varphi_+(\omega)$, $\varphi_-(\omega)$, $g_+(\omega)$ and $g_-(\omega)$ are presented as

$$\begin{aligned}\varphi_+(\omega) &= \frac{\omega}{\omega_0^2} e^{-\omega/\omega_0}, & \varphi_-(\omega) &= \left\{ \frac{1}{\omega_0} - \frac{\lambda_E^2 - \lambda_H^2}{9\omega_0^3} \left[1 - 2\left(\frac{\omega}{\omega_0}\right) + \frac{1}{2}\left(\frac{\omega}{\omega_0}\right)^2 \right] \right\} e^{-\omega/\omega_0}, \\ g_+(\omega) &= \frac{15}{32\omega_0} \omega^2 e^{-\omega/\omega_0}, & g_-(\omega) &= \left\{ \frac{3}{4} - \frac{\lambda_E^2 - \lambda_H^2}{12\omega_0^3} \left[1 - \left(\frac{\omega}{\omega_0}\right) + \frac{1}{3}\left(\frac{\omega}{\omega_0}\right)^2 \right] \right\} \omega e^{-\omega/\omega_0}.\end{aligned}\quad (13)$$

The values of the parameters λ_E^2 and λ_H^2 of the B -meson DAs are chosen as $\lambda_E^2 = (0.01 \pm 0.01) \text{ GeV}^2$ and $\lambda_H^2 = (0.15 \pm 0.05) \text{ GeV}^2$ [42]. Implementing the EOM constraint for the Exp model leads to $\omega_0 = \lambda_{B_{(s)}}$ [43]. Prediction of the λ_B and λ_{B_s} values are varied in different models [27,44,45]. In this work, we use the values for λ_B and λ_{B_s} based on the recent researches. Analyzing the $\bar{B}_u \rightarrow \gamma l^- \bar{\nu}$ decay by the LCSR leads to $\lambda_B = (360 \pm 110) \text{ MeV}$ [46]. On the other hand,

the inverse moment of the B_s -meson DA is predicted from the QCDSR as $\lambda_{B_s} = (438 \pm 150) \text{ MeV}$ [47]. Therefore

$$\omega_0 = \begin{cases} \lambda_B = 0.360 \pm 0.110 \text{ GeV} & (\text{For } B\text{-meson}), \\ \lambda_{B_s} = 0.438 \pm 0.150 \text{ GeV} & (\text{For } B_s\text{-meson}). \end{cases}\quad (14)$$

The dependence of the two-particle DAs in Eq. (13) with respect to ω is shown in Fig. 1 for the Exp model.

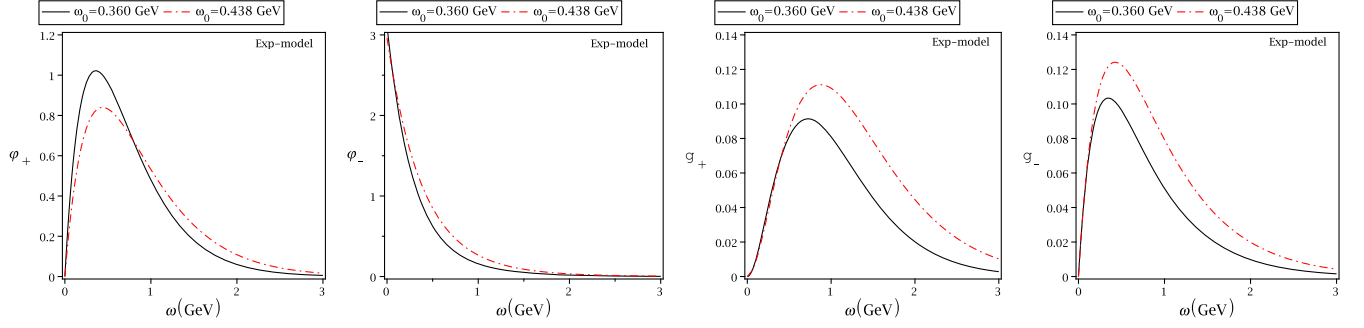


FIG. 1. The dependence of the two-particle DAs, $\varphi_+(\omega)$, $\varphi_-(\omega)$, $g_+(\omega)$, and $g_-(\omega)$ on ω for the Exp model.

The three-particle DAs of the B meson up to twist-six in the Exp model can be constructed as

$$\begin{aligned}
 \phi_3(\omega, \xi) &= \frac{\lambda_E^2 - \lambda_H^2}{6\omega_0^5} \omega \xi^2 e^{-(\omega+\xi)/\omega_0}, & \phi_4(\omega, \xi) &= \frac{\lambda_E^2 + \lambda_H^2}{6\omega_0^4} \xi^2 e^{-(\omega+\xi)/\omega_0}, \\
 \psi_4(\omega, \xi) &= \frac{\lambda_E^2}{3\omega_0^4} \omega \xi e^{-(\omega+\xi)/\omega_0}, & \bar{\psi}_4(\omega, \xi) &= \frac{\lambda_H^2}{3\omega_0^4} \omega \xi e^{-(\omega+\xi)/\omega_0}, \\
 \psi_5(\omega, \xi) &= -\frac{\lambda_E^2}{3\omega_0^3} \xi e^{-(\omega+\xi)/\omega_0}, & \bar{\psi}_5(\omega, \xi) &= -\frac{\lambda_H^2}{3\omega_0^3} \xi e^{-(\omega+\xi)/\omega_0}, \\
 \phi_5(\omega, \xi) &= \frac{\lambda_E^2 + \lambda_H^2}{3\omega_0^3} \omega e^{-(\omega+\xi)/\omega_0}, & \phi_6(\omega, \xi) &= \frac{\lambda_E^2 - \lambda_H^2}{3\omega_0^2} e^{-(\omega+\xi)/\omega_0}.
 \end{aligned} \tag{15}$$

B. LD model

Another class of the phenomenological models for the B -meson DAs is the LD model. In this model, the structures of the two-particle DAs $\varphi_+(\omega)$, $\varphi_-(\omega)$, $g_+(\omega)$ and $g_-(\omega)$ are presented as [31]

$$\begin{aligned}
 \varphi_+(\omega) &= \frac{5}{8\omega_0^5} \omega (2\omega_0 - \omega)^3 \theta(2\omega_0 - \omega), \\
 \varphi_-(\omega) &= \frac{5(2\omega_0 - \omega)^2}{192\omega_0^5} \left\{ 6(2\omega_0 - \omega)^2 - \frac{7(\lambda_E^2 - \lambda_H^2)}{\omega_0^2} (15\omega^2 - 20\omega\omega_0 + 4\omega_0^2) \right\} \theta(2\omega_0 - \omega), \\
 g_+(\omega) &= \frac{115}{2048\omega_0^5} \omega^2 (2\omega_0 - \omega)^4 \theta(2\omega_0 - \omega), \\
 g_-(\omega) &= \frac{\omega(2\omega_0 - \omega)^3}{\omega_0^5} \left\{ \frac{5}{256} (2\omega_0 - \omega)^2 - \frac{35(\lambda_E^2 - \lambda_H^2)}{1536} \left[4 - 12 \left(\frac{\omega}{\omega_0} \right) + 11 \left(\frac{\omega}{\omega_0} \right)^2 \right] \right\} \theta(2\omega_0 - \omega).
 \end{aligned} \tag{16}$$

Applying the EOM constraint between the leading-twist and the higher-twist B -meson DAs, the HQET parameters entering the LD model for the $B_{(s)}$ -meson DAs must satisfy the relation $\omega_0 = \frac{5}{2} \lambda_{B_{(s)}}$ [31]. So according to Eq. (14), we have

$$\omega_0 = \begin{cases} \lambda_B = 0.900 \pm 0.275 \text{ GeV} & (\text{For } B \text{ - meson}), \\ \lambda_{B_s} = 1.095 \pm 0.375 \text{ GeV} & (\text{For } B_s \text{ - meson}). \end{cases} \tag{17}$$

The dependence of the two-particle DAs in Eq. (16) with respect to ω is shown in Fig. 2 for the LD model.

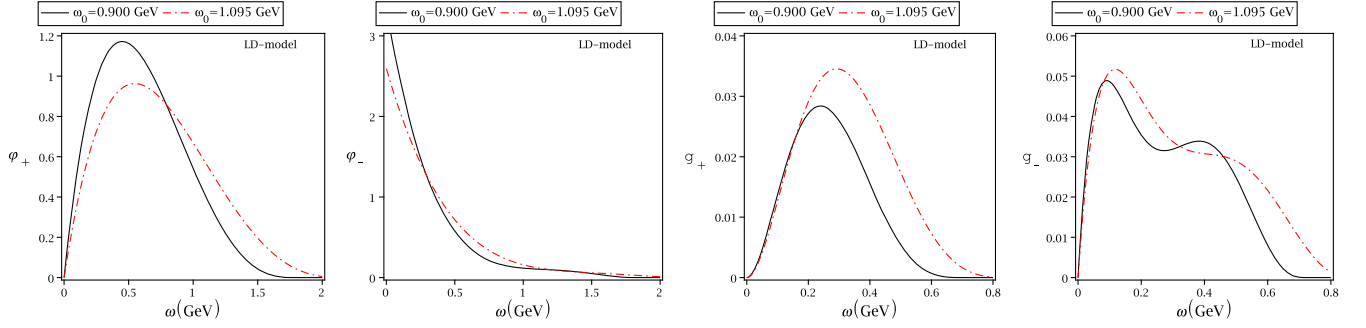


FIG. 2. The same as Fig. 1 but for the LD model.

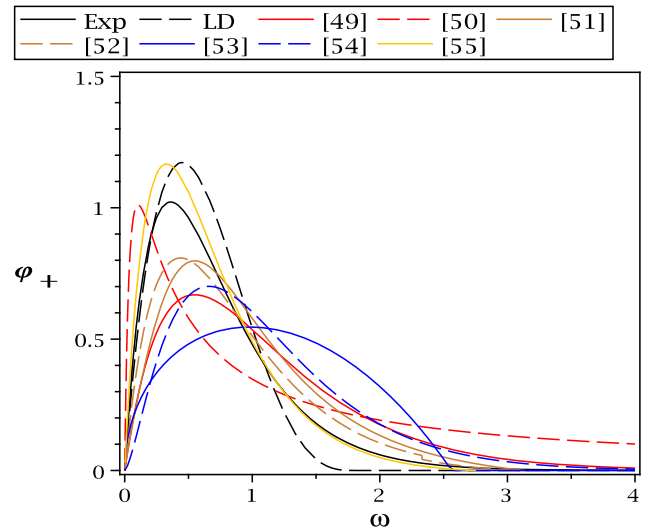
The three-particle DAs of the B meson are derived in the LD model up to twist-six as [31,32]

$$\begin{aligned}\phi_3(\omega, \xi) &= \frac{105(\lambda_E^2 - \lambda_H^2)}{8\omega_0^7} \omega \xi^2 \left(\omega_0 - \frac{\omega + \xi}{2} \right)^2 \theta(2\omega_0 - \omega - \xi), \\ \phi_4(\omega, \xi) &= \frac{35(\lambda_E^2 + \lambda_H^2)}{4\omega_0^7} \xi^2 \left(\omega_0 - \frac{\omega + \xi}{2} \right)^3 \theta(2\omega_0 - \omega - \xi), \\ \psi_4(\omega, \xi) &= \frac{35\lambda_E^2}{2\omega_0^7} \omega \xi \left(\omega_0 - \frac{\omega + \xi}{2} \right)^3 \theta(2\omega_0 - \omega - \xi), \\ \bar{\psi}_4(\omega, \xi) &= \frac{35\lambda_H^2}{2\omega_0^7} \omega \xi \left(\omega_0 - \frac{\omega + \xi}{2} \right)^3 \theta(2\omega_0 - \omega - \xi), \\ \phi_5(\omega, \xi) &= \frac{35(\lambda_E^2 + \lambda_H^2)}{64\omega_0^7} \omega (2\omega_0 - \omega - \xi)^4 \theta(2\omega_0 - \omega - \xi), \\ \psi_5(\omega, \xi) &= -\frac{35\lambda_E^2}{64\omega_0^7} \xi (2\omega_0 - \omega - \xi)^4 \theta(2\omega_0 - \omega - \xi), \\ \bar{\psi}_5(\omega, \xi) &= -\frac{35\lambda_H^2}{64\omega_0^7} \xi (2\omega_0 - \omega - \xi)^4 \theta(2\omega_0 - \omega - \xi), \\ \phi_6(\omega, \xi) &= \frac{7(\lambda_E^2 - \lambda_H^2)}{64\omega_0^7} (2\omega_0 - \omega - \xi)^5 \theta(2\omega_0 - \omega - \xi). \quad (18)\end{aligned}$$

The two-particle leading-twist DA of the B meson $\varphi_+(\omega)$ has the most important contribution in the estimation of the form factors. The evolution effects show that the DA $\varphi_+(\omega)$ satisfies the condition $\varphi_+(\omega) \sim \omega$ as $\omega \rightarrow 0$ and falls off slower than $1/\omega$ for $\omega \rightarrow \infty$ [48]. In Fig. 3, the shape of $\varphi_+(\omega)$ in the Exp and LD models is compared with those proposed by other models in Refs. [49–55].

After introducing the DAs of the B meson, we set the values of the parameters. There are two auxiliary parameters in Eq. (11), the Borel mass square M^2 and the continuum threshold s_0 , the values of which must be determined before analyzing the form factors of the semileptonic $B_{(s)} \rightarrow S$ decays. These parameters are not physical quantities, so the form factors as physical quantities should be independent of them. The continuum threshold s_0 is not completely arbitrary and it is related to the energy of the first excited state of the scalar meson.

The working region for the continuum threshold for the scalar mesons $K_0^*(1430)$, $a_0(1450)$ and $f_0(1500)$ is taken to be $s_0 = (4.4 \pm 0.4) \text{ GeV}^2$ [56]. The Borel parameter M^2 is chosen in the region where (a) the contributions of the higher states and continuum are effectively suppressed, which can ensure that the sum rule does not sensitively depend on the approximation for the higher states and continuum, and (b) the contributions of the condensates should not be too large, which can ensure that the contributions of the higher-dimensional operators are small and the truncated OPE is effective. Considering the central value 4.4 GeV^2 for s_0 , a good stability of the form factors with respect to the Borel parameter is obtained at $q^2 = 0$ in the interval $2.5 \text{ GeV}^2 \leq M^2 \leq 3.5 \text{ GeV}^2$. The dependence of the form factors f_+ , f_- and f_T for the semileptonic decays $B \rightarrow (a_0, K_0^*)$ and $B_s \rightarrow (K_0^*, f_0)$ on the Borel parameter M^2 at three fixed values of the continuum threshold i.e., $s_0 = 4.0, 4.4$ and 4.8 , and $q^2 = 0$ is shown in Figs. 4 and 5 through the two Exp and LD models, respectively. We take $M^2 = 3 \text{ GeV}^2$ in our calculations.

FIG. 3. The shape of $\varphi_+(\omega)$ for the B meson in the Exp and LD and other models.

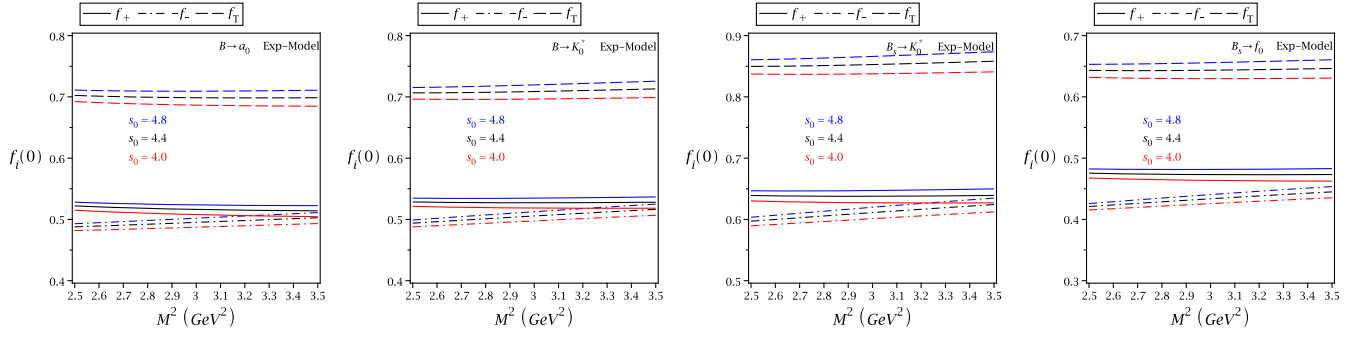


FIG. 4. The dependence of the form factors f_+ , $-f_-$ and f_T on the Borel parameter M^2 at three fixed values $s_0 = 4.0, 4.4$, and 4.8 for $B \rightarrow (a_0, K_0^*)$ and $B_s \rightarrow (K_0^*, f_0)$ at $q^2 = 0$ in the Exp model.

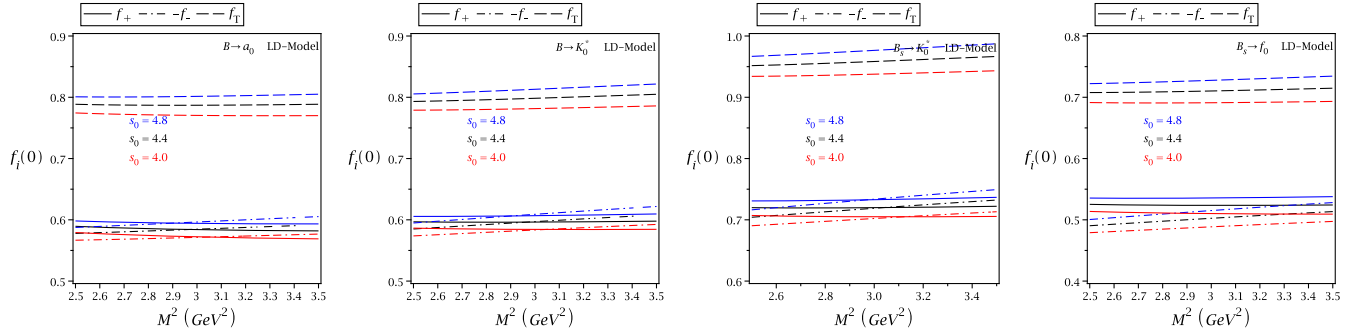


FIG. 5. The same as Fig. 4 but for the LD model.

C. Form factor analysis

Inserting the values of the masses, the leptonic decay constants f_S and $f_{B_{(S)}}$, the continuum threshold s_0 , the Borel parameter M^2 , the B -meson DAs and other quantities and parameters related to them such as ω_0 , λ_E^2 and λ_H^2 , in addition considering all sources of uncertainties, the central values of the form factors f_+ , f_- , and f_T and also their errors can be estimated for the semileptonic decays $B_{(s)} \rightarrow (K_0^*, a_0, f_0)$ at $q^2 = 0$ via the B -meson LCSR approach. Our results for the form factors at $q^2 = 0$ using the B -meson DAs through the

$$f_+^{B \rightarrow a_0}(0) = 0.52^{+0.21}_{-0.13} \Big|_{\delta\omega_0} +0.06 \Big|_{\delta f_{a_0}} +0.01 \Big|_{\delta s_0} +0.00 \Big|_{\delta\lambda_H^2} +0.00 \Big|_{\delta M^2} +0.00 \Big|_{\delta m_{a_0}} +0.00 \Big|_{\delta\lambda_E^2}. \quad (19)$$

As the calculations show, the most value of error for f_+ enters through the variation of ω_0 .

Table II shows that considering the uncertainties, there is a good agreement between our results in the Exp model and predictions of the conventional LCSR in S2 [21,24] for all cases. As a result, our calculations confirm scenario 2 for describing the scalar mesons $K_0^*(1430)$, $a_0(1450)$, and $f_0(1500)$. This means that the scalar mesons $K_0^*(1430)$, $a_0(1450)$, and $f_0(1500)$ can be seen as the lowest lying states with two quarks in the quark model.

two Exp and LD models, as well as the predictions of other approaches such as the pQCD [14], CLF [15], QCDSR [16–18], LFQM [19], MSSM [20], and the LCSR with the light-meson DAs [21,24,26] are collected in Table II. The most important sources of uncertainties in our calculations are ω_0 and then the decay constants of the light mesons. For example, considering the form factor f_+ of the semileptonic decay $B \rightarrow a_0$, and taking into account the variation of the input values and parameters, we obtain the following results in the Exp model:

Table III shows the individual contributions of the two- and three-particle DAs to the semileptonic form factors $B_{(s)} \rightarrow (K_0^*, a_0, f_0)$ at $q^2 = 0$. Note that the contributions of the two-particle DAs are listed based on twist level φ_+ , φ_- , and g_+ , while g_- does not appear in the results of the form factors. As can be seen, the two-particle leading-twist DA of the B meson φ_+ has the most important contribution in the calculation of the form factors. In this table, the higher-twist contributions of the three-particle DAs are not presented separately because their contributions are usually less than 0.01. For instance, the contributions of the eight twist

TABLE II. The form factors of the semileptonic $B_{(s)} \rightarrow (K_0^*, a_0, f_0)$ transitions at zero momentum transfer from different approaches.

Decay mode	Method	Reference	$f_+(0)$	$f_-(0)$	$f_T(0)$
$B \rightarrow a_0$	LCSR(Exp model)	Ours	$0.52^{+0.28}_{-0.23}$	$-0.50^{+0.13}_{-0.35}$	$0.71^{+0.37}_{-0.30}$
	LCSR(LD model)	Ours	$0.58^{+0.38}_{-0.23}$	$-0.58^{+0.29}_{-0.37}$	$0.78^{+0.44}_{-0.35}$
	LCSR	[26]	0.44	-0.26	0.43
	LCSR(S2)	[21]	0.52	-0.44	0.66
	LCSR(S2)	[24]	0.53	-0.53	...
	pQCD(S2)	[14]	0.68	...	0.92
	LCSR(S1)	[24]	0.26	-0.26	...
	pQCD(S1)	[14]	-0.31	...	-0.41
	CLF	[15]	0.26
$B \rightarrow K_0^*$	LCSR(Exp model)	Ours	$0.53^{+0.28}_{-0.22}$	$-0.51^{+0.13}_{-0.36}$	$0.72^{+0.39}_{-0.31}$
	LCSR(LD model)	Ours	$0.60^{+0.34}_{-0.28}$	$-0.59^{+0.30}_{-0.41}$	$0.79^{+0.45}_{-0.35}$
	LCSR	[26]	0.45	-0.28	0.46
	LCSR(S2)	[21]	0.49	-0.41	0.60
	LCSR(S2)	[24]	0.49	-0.49	0.69
	pQCD(S2)	[14]	0.60	...	0.78
	LCSR(S1)	[24]	0.17	-0.17	0.24
	pQCD(S1)	[14]	-0.34	...	-0.44
	CLF	[15]	0.26
	QCDSR	[16]	0.31	-0.31	-0.26
	LFQM	[19]	-0.26	0.21	-0.34
	MSSM	[20]	0.49	-0.41	0.60
$B_s \rightarrow K_0^*$	LCSR(Exp model)	Ours	$0.51^{+0.38}_{-0.24}$	$-0.48^{+0.24}_{-0.40}$	$0.70^{+0.50}_{-0.32}$
	LCSR(LD model)	Ours	$0.56^{+0.48}_{-0.27}$	$-0.54^{+0.34}_{-0.50}$	$0.75^{+0.59}_{-0.37}$
	LCSR	[26]	0.39	-0.25	0.41
	LCSR(S2)	[21]	0.42	-0.34	0.52
	LCSR(S2)	[24]	0.44	-0.44	...
	pQCD(S2)	[14]	0.56	...	0.72
	LCSR(S1)	[24]	0.10	-0.10	...
	pQCD(S1)	[14]	-0.32	...	-0.41
	QCDSR	[17]	0.24
	QCDSR	[18]	0.25	-0.17	0.21
$B_s \rightarrow f_0$	LCSR(Exp model)	Ours	$0.47^{+0.36}_{-0.20}$	$-0.45^{+0.22}_{-0.35}$	$0.66^{+0.44}_{-0.31}$
	LCSR(LD model)	Ours	$0.52^{+0.43}_{-0.24}$	$-0.50^{+0.28}_{-0.47}$	$0.71^{+0.51}_{-0.38}$
	LCSR	[26]	0.38	-0.24	0.40
	LCSR(S2)	[21]	0.43	-0.37	0.56
	LCSR(S2)	[24]	0.41	-0.41	0.59
	pQCD(S2)	[14]	0.60	...	0.82
	LCSR(S1)	[24]	0.14	-0.14	0.20
	pQCD(S1)	[14]	-0.26	...	-0.34

functions $\Psi_A, \Psi_V, X_A, Y_A, \bar{X}_A, \bar{Y}_A, W$, and Z for the form factor $f_+^{B \rightarrow a_0}$ at $q^2 = 0$ are reported in Table IV in the Exp model.

Because of the cutoff in QCD theories, the form factors for each aforementioned semileptonic decay can be estimated by the B -meson LCSR method in nearly half of the physical region $0 \leq q^2 \leq (m_{B_{(s)}} - m_S)^2$. In order to extend our results to the full physical region, we look for a parametrization of the form factors in such a way that in the validity region of the LCSR, this parametrization coincides with the LCSR predictions. We use the following fit functions of the form factors with respect to q^2 as

$$f^I(q^2) = \frac{f(0)}{1 - \alpha s + \beta s^2},$$

$$f^{II}(q^2) = \frac{1}{1-s} \sum_{k=0}^2 b_k [z(q^2) - z(0)]^k, \quad (20)$$

where $s = q^2/m_{B_{(s)}}^2$, $z(t) = \frac{\sqrt{t_+ - t} - \sqrt{t_+ - t_0}}{\sqrt{t_+ - t} + \sqrt{t_+ - t_0}}$, $t_0 = t_+(1 - \sqrt{1 - t_-/t_+})$, and $t_{\pm} = (m_{B_{(s)}} \pm m_S)^2$. The parameters $(f(0), \alpha, \beta)$ and (b_0, b_1, b_2) , related to the fit functions $f^I(q^2)$ and $f^{II}(q^2)$ respectively, are determined from the fitting procedure. Table V shows the values of these

TABLE III. Contributions of the two-particle DAs (2-P DAs) and three-particle DAs (3-P DAs) to the form factor results at $q^2 = 0$ in the two Exp and LD models.

Form Factor	Exp model				LD model			
	2-P DAs		3-P DAs		2-P DAs		3-P DAs	
	φ_+	φ_-	g_+	3-P DAs	φ_+	φ_-	g_+	3-P DAs
$f_+^{B \rightarrow a_0}$	0.49	0.07	-0.05	0.01	0.52	0.08	-0.04	0.02
$f_-^{B \rightarrow a_0}$	-0.61	0.07	0.05	-0.01	-0.68	0.08	0.04	-0.02
$f_T^{B \rightarrow a_0}$	0.70	0.00	0.00	0.01	0.77	0.00	0.00	0.01
$f_+^{B \rightarrow K_0^*}$	0.50	0.07	-0.05	0.01	0.54	0.08	-0.04	0.02
$f_-^{B \rightarrow K_0^*}$	-0.63	0.07	0.06	-0.01	-0.69	0.08	0.04	-0.02
$f_T^{B \rightarrow K_0^*}$	0.71	0.00	0.00	0.01	0.78	0.00	0.00	0.01
$f_+^{B_s \rightarrow K_0^*}$	0.48	0.08	-0.06	0.01	0.51	0.08	-0.05	0.02
$f_-^{B_s \rightarrow K_0^*}$	-0.62	0.08	0.07	-0.01	-0.66	0.08	0.06	-0.02
$f_T^{B_s \rightarrow K_0^*}$	0.69	0.00	0.00	0.01	0.74	0.00	0.00	0.01
$f_+^{B_s \rightarrow f_0}$	0.44	0.07	-0.05	0.01	0.46	0.08	-0.04	0.02
$f_-^{B_s \rightarrow f_0}$	-0.57	0.07	0.06	-0.01	-0.61	0.08	0.05	-0.02
$f_T^{B_s \rightarrow f_0}$	0.65	0.00	0.00	0.01	0.70	0.00	0.00	0.01

TABLE IV. Contributions of the eight twist functions $\Psi_A, \Psi_V, X_A, Y_A, \bar{X}_A, \bar{Y}_A, W,$ and Z for the form factor $f_+^{B \rightarrow a_0}$ at $q^2 = 0$ up to $\mathcal{O}(10^{-3})$ in the Exp model.

	Ψ_A	Ψ_V	X_A	Y_A	\bar{X}_A	\bar{Y}_A	W	Z
$f_+^{B \rightarrow a_0}$	-0.002	0.015	-0.002	0.001	0.000	0	-0.001	-0.001

parameters for the form factors of the semileptonic decays $B_{(S)} \rightarrow (K_0^*, a_0, f_0)$ in the Exp model. Table VI shows the same values as Table V but for the LD model.

The dependence of the fitted form factors $f_i (i = +, -, T)$ on q^2 is given in Fig. 6 for $B_{(S)} \rightarrow S (S = K_0^*, a_0, f_0)$ transitions. These form factors are related to the Exp model. Figure 7 depicts the same results as Fig. 6, but for the LD model. In these figures, the black and gray lines show the results for $f^I(q^2)$ and $f^{II}(q^2)$ fit functions, respectively. According to Figs. 6 and 7, the fitted form factors obtained for the two fit functions are consistent in each case.

The form factors at large recoil should satisfy the following relations [57]:

$$f_-(q^2) = -\frac{m_{B_{(S)}}^2 - m_S^2}{m_b m_{B_{(S)}}} f_+(q^2),$$

$$f_T(q^2) = \frac{m_{B_{(S)}} + m_S}{m_{B_{(S)}}} f_+(q^2). \quad (21)$$

Figures 6 and 7 show that the computed form factors from the LCSR with the B -meson DAs for the two Exp and LD models satisfy the relations in Eq. (21), by considering the errors.

TABLE V. Values of parameters $(f(0), \alpha, \beta)$ and (b_0, b_1, b_2) connected to the fit functions $f^I(q^2)$ and $f^{II}(q^2)$ respectively, for the fitted form factors of $B_{(S)} \rightarrow (K_0^*, a_0, f_0)$ transitions in the Exp model.

Form factor	$f(0)$	α	β	b_0	b_1	b_2
$f_+^{B \rightarrow a_0}$	0.52	-0.49	1.68	0.52	-0.23	-6.83
$f_-^{B \rightarrow a_0}$	-0.50	0.44	-1.51	-0.50	0.54	5.41
$f_T^{B \rightarrow a_0}$	0.71	-0.59	2.53	0.71	-0.95	-3.79
$f_+^{B \rightarrow K_0^*}$	0.53	-0.50	1.71	0.53	-0.23	-6.79
$f_-^{B \rightarrow K_0^*}$	-0.51	0.44	-1.55	-0.51	0.55	5.39
$f_T^{B \rightarrow K_0^*}$	0.72	-0.60	2.57	0.72	-0.95	-3.77
$f_+^{B_s \rightarrow K_0^*}$	0.51	-0.43	1.51	0.51	-0.65	-4.46
$f_-^{B_s \rightarrow K_0^*}$	-0.48	0.38	-1.37	-0.48	0.89	2.32
$f_T^{B_s \rightarrow K_0^*}$	0.70	-0.51	2.25	0.70	-1.65	2.99
$f_+^{B_s \rightarrow f_0}$	0.47	-0.39	1.10	0.47	-0.69	-6.15
$f_-^{B_s \rightarrow f_0}$	-0.45	0.36	-1.34	-0.45	0.75	2.53
$f_T^{B_s \rightarrow f_0}$	0.66	-0.48	2.11	0.66	-1.58	3.05

TABLE VI. The same as Table V but for the LD model.

Form factor	$f(0)$	α	β	b_0	b_1	b_2
$f_+^{B \rightarrow a_0}$	0.58	-0.48	0.95	0.58	-0.86	-13.82
$f_-^{B \rightarrow a_0}$	-0.58	0.42	-0.83	-0.58	1.49	11.43
$f_T^{B \rightarrow a_0}$	0.78	-0.58	1.15	0.78	-1.82	-16.30
$f_+^{B \rightarrow K_0^*}$	0.60	-0.49	0.97	0.60	-0.87	-13.77
$f_-^{B \rightarrow K_0^*}$	-0.59	0.43	-0.85	-0.59	1.50	11.41
$f_T^{B \rightarrow K_0^*}$	0.79	-0.59	1.16	0.79	-1.83	-16.15
$f_+^{B_s \rightarrow K_0^*}$	0.56	-0.41	1.07	0.56	-1.44	-4.24
$f_-^{B_s \rightarrow K_0^*}$	-0.54	0.35	-0.93	-0.54	1.94	-2.27
$f_T^{B_s \rightarrow K_0^*}$	0.75	-0.49	1.26	0.75	-2.67	1.49
$f_+^{B_s \rightarrow f_0}$	0.52	-0.38	1.00	0.52	-1.36	-4.07
$f_-^{B_s \rightarrow f_0}$	-0.50	0.32	-0.86	-0.50	1.85	-2.33
$f_T^{B_s \rightarrow f_0}$	0.71	-0.46	1.19	0.71	-2.56	1.62

The results of the form factor $f_+(q^2)$ for the aforementioned decays from different models are compared with our results in the two Exp and LD models in Fig. 8.

D. Semileptonic $B_s^0 \rightarrow K_0^{*+} l^- \bar{\nu}_l$ and $B^0 \rightarrow a_0^+ l^- \bar{\nu}_l$ decays

At the quark level, the tree-level $b \rightarrow u$ transition is responsible for the $B_s \rightarrow K_0^* l \bar{\nu}_l$ and $B \rightarrow a_0 l \bar{\nu}_l$ decay modes. The Hamiltonian for the $b \rightarrow ul \bar{\nu}_l$ transition is written as

$$\mathcal{H}_{\text{eff}}(b \rightarrow ul \bar{\nu}_l) = \frac{G_F}{\sqrt{2}} V_{ub} \bar{u} \gamma_\mu (1 - \gamma_5) b \bar{l} \gamma^\mu (1 - \gamma_5) \nu_l, \quad (22)$$

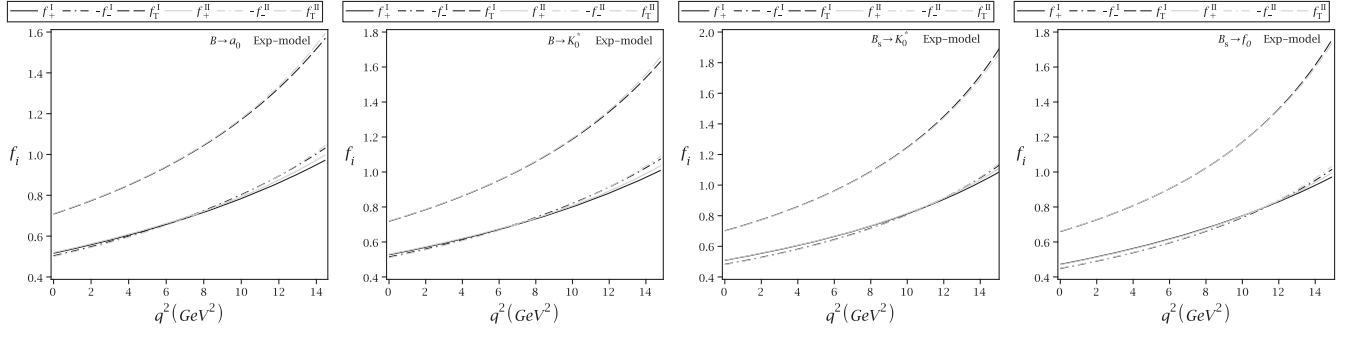


FIG. 6. Black and gray lines show the fitted form factors f_+ , $-f_-$, and f_T of the $B_{(s)} \rightarrow S$ transitions by using the fit functions $f^I(q^2)$ and $f^{II}(q^2)$, respectively, with respect to q^2 in the Exp model.

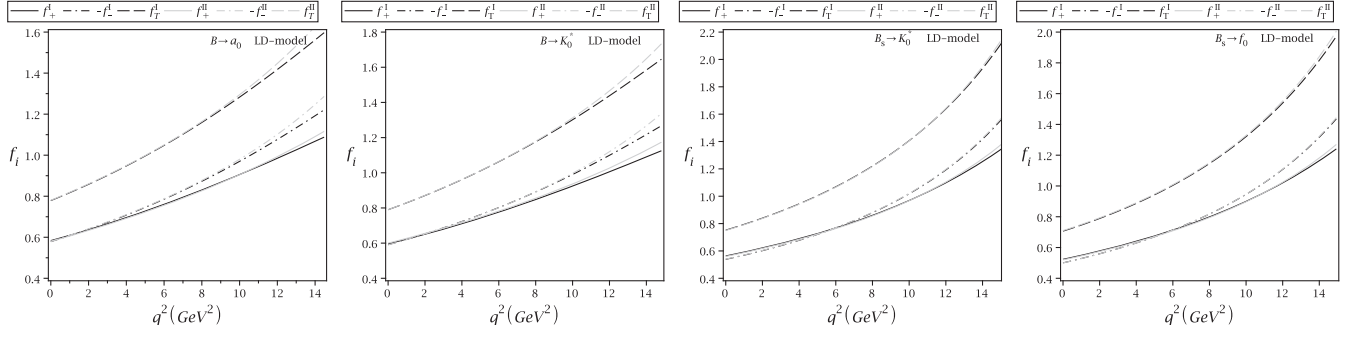


FIG. 7. The same as Fig. 6 but for the LD model.

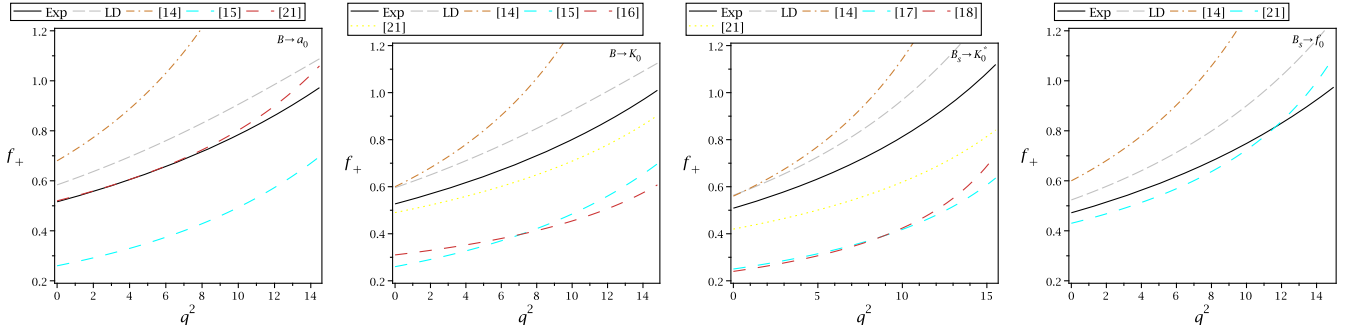


FIG. 8. Form factor f_+ for $B \rightarrow (a_0, K_0^*)$ and $B_s \rightarrow (K_0^*, f_0)$ decays in different models such as the pQCD [14], CLF [15], QCDSR [16–18], the LCSR with the light-meson DAs [21] and our results via B -meson LCSR in two Exp and LD models.

where G_F is the Fermi constant, $V_{ub} = (3.82 \pm 0.24) \times 10^{-3}$. With this Hamiltonian, the differential decay width $\frac{d\Gamma}{dq^2}$ for the processes $B_{(s)} \rightarrow S l \bar{\nu}_l$ ($S = K_0^*, a_0$) in terms of the form factors can be expressed as [58]

$$\begin{aligned} \frac{d\Gamma}{dq^2}(B_{(s)} \rightarrow S l \bar{\nu}_l) &= \frac{G_F^2 |V_{ub}|^2}{384\pi^3 m_{B_{(s)}}^3} \frac{(q^2 - m_l^2)^2}{(q^2)^3} \sqrt{(m_{B_{(s)}}^2 - m_S^2 - q^2)^2 - 4q^2 m_S^2} \left\{ (m_l^2 + 2q^2) \right. \\ &\quad \left. \times \sqrt{(m_{B_{(s)}}^2 - m_S^2 - q^2)^2 - 4q^2 m_S^2} f_+^2(q^2) + 3m_l^2 (m_{B_{(s)}}^2 - m_S^2) \left[f_+(q^2) + \frac{q^2}{m_{B_{(s)}}^2 - m_S^2} f_-(q^2) \right]^2 \right\}, \quad (23) \end{aligned}$$

where m_l is the mass of the lepton. The dependency of the differential branching ratios of $B_s \rightarrow K_0^* l \bar{\nu}_l$ and $B \rightarrow a_0 l \bar{\nu}_l$ ($l = \mu, \tau$) decays on q^2 is shown in Fig. 9 for both the Exp and LD models as well as the two fit functions $f^I(q^2)$ and $f^{II}(q^2)$.

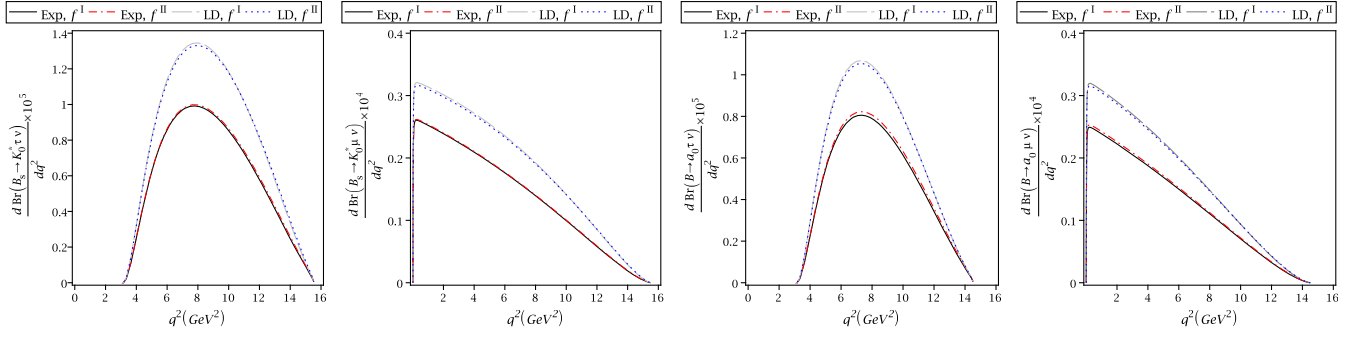


FIG. 9. Differential branching ratios of the semileptonic $B_{(S)} \rightarrow (K_0^*, a_0) l \nu$ ($l = \mu, \tau$) transitions on q^2 for the Exp model and fit function $f^I(q^2)$ (Exp, f^I), the Exp model and fit function $f^{II}(q^2)$ (Exp, f^{II}), the LD model and fit function $f^I(q^2)$ (LD, f^I), and the LD model and fit function $f^{II}(q^2)$ (LD, f^{II}).

Integrating Eq. (23) over q^2 in the whole physical region $m_l^2 \leq q^2 \leq (m_{B_{(S)}} - m_S)^2$, and using the total mean lifetimes $\tau_{B_s} = (1.515 \pm 0.004) ps$ and $\tau_{B^0} = (1.519 \pm 0.004) ps$ [36], we present the branching ratio values of the semileptonic decays $B_{(S)} \rightarrow (K_0^*, a_0) l \bar{\nu}_l$ ($l = \mu, \tau$) in Table VII, for both the Exp and LD models, in addition the two fit functions. The results obtained for the electron are very close to the results of the muon. Therefore, the branching ratios for muon are only presented in this table. Table VII shows that the difference between the calculations through the two fit functions can be completely ignored. This table also contains the results estimated via the conventional LCSR [21] and pQCD [14] through S2 as well as the QCDSR [17] approach. In general, the values obtained in this work are in a logical agreement with the two models, the conventional LCSR and pQCD. Especially, the obtained values of the Exp model are in a good agreement with the conventional LCSR. As can be seen in this table, uncertainties in the values obtained for the branching ratios of the semileptonic decays are very large. The main source of errors comes from the form factor $f_+(q^2)$.

E. Semileptonic $B^0 \rightarrow K_0^* l^+ l^- / \nu \bar{\nu}$ and $B_s^0 \rightarrow f_0^* l^+ l^- / \nu \bar{\nu}$ decays

The semileptonic decays $B_{(S)} \rightarrow (K_0^*, f_0) l^+ l^- / \nu \bar{\nu}$ are conducted by the FCNC $b \rightarrow s$ loop transition. In the

SM, the weak effective Hamiltonian responsible for these rare decays, neglecting the Cabibbo-Kobayashi-Maskawa-suppressed contributions proportional to $V_{ub} V_{us}^*$, and also considering the approximation $|V_{tb} V_{ts}| \simeq |V_{cb} V_{cs}|$, is described at the energy scale $\mu = m_b$ as [59–61]:

$$\mathcal{H}_{\text{eff}}(b \rightarrow s l^+ l^-) = -\frac{4G_F}{\sqrt{2}} V_{tb} V_{ts}^* \left(C_1 O_1^c + C_2 O_2^c + \sum_{i=3}^{10} C_i O_i \right), \quad (24)$$

where $C_i(\mu)$ are the Wilson coefficients. $O_{1,2}^c$ are current-current operators, O_{3-6} are QCD penguin operators, $O_{7,8}$ are magnetic penguin operators, and $O_{9,10}$ are semileptonic electroweak penguin operators. The contributions of the operators O_7 and $O_{9,10}$ in the decay amplitudes $B_{(S)} \rightarrow (K_0^*, f_0)$ are factorized in the form factors f_{\pm} and f_T . The effect of other operators appears as the factorizable and nonfactorizable contributions.

The factorizable contributions have the same form factor dependence as C_9 which can be absorbed into an effective Wilson coefficient C_9^{eff} . The dominant factorizable contribution is generated by the tree-level four quark operators $O_{1,2}^c$ with large Wilson coefficients $|V_{cb} V_{cs}|$. This contribution includes intermediate vector charmonium states in the upper part of the decay kinematical region as long-distance effect.

TABLE VII. The branching ratio values of $B_{(S)} \rightarrow (K_0^*, a_0) l \bar{\nu}_l$ for both the Exp and LD models as well as the two fit functions in addition different approaches.

Mode	This work				LCSR(S2) [21]	pQCD(S2) [14]	QCDSR [17]
	Exp, f^I	Exp, f^{II}	LD, f^I	LD, f^{II}			
$\text{Br}(B_s \rightarrow K_0^* \mu \nu_\mu) \times 10^4$	$1.98_{-0.65}^{+1.51}$	$2.00_{-0.66}^{+1.52}$	$2.63_{-0.87}^{+1.99}$	$2.60_{-0.86}^{+1.98}$	$1.30_{-0.40}^{+1.30}$	$2.45_{-1.05}^{+1.77}$	$0.36_{-0.24}^{+0.38}$
$\text{Br}(B_s \rightarrow K_0^* \tau \nu_\tau) \times 10^4$	$0.70_{-0.26}^{+0.57}$	$0.71_{-0.27}^{+0.58}$	$0.95_{-0.35}^{+0.77}$	$0.95_{-0.35}^{+0.77}$	$0.52_{-0.18}^{+0.57}$	$1.09_{-0.47}^{+0.82}$...
$\text{Br}(B \rightarrow a_0 \mu \nu_\mu) \times 10^4$	$1.67_{-0.53}^{+1.27}$	$1.70_{-0.54}^{+1.29}$	$2.20_{-0.70}^{+1.67}$	$2.18_{-0.69}^{+1.66}$	$1.80_{-0.70}^{+1.66}$	$3.25_{-1.36}^{+2.36}$...
$\text{Br}(B \rightarrow a_0 \tau \nu_\tau) \times 10^4$	$0.51_{-0.19}^{+0.41}$	$0.53_{-0.20}^{+0.42}$	$0.67_{-0.25}^{+0.54}$	$0.66_{-0.24}^{+0.53}$	$0.63_{-0.25}^{+0.34}$	$1.32_{-0.57}^{+0.97}$...

The nonfactorizable contributions arise from electromagnetic corrections to the matrix elements of purely hadronic operators in the weak effective Hamiltonian. The weak annihilation and quark-loop diagrams with soft and hard gluons create the nonfactorizable corrections [61,62]. These contributions for the FCNC $B_{(s)} \rightarrow (K_0^*, f_0)$ decays are highly suppressed due to the large current uncertainties of the form factors, and

also the small Wilson coefficients of the penguin operators.

According to the effective weak Hamiltonian of the $b \rightarrow sl^+l^-$ transition in Eq. (24), the matrix element for this FCNC decay, by considering the contributions of the operators O_7 and $O_{9,10}$ as well as the factorizable contributions of the operators through C_9^{eff} , and ignoring the nonfactorizable contributions, can be written as

$$\mathcal{M}(b \rightarrow sl^+l^-) = \frac{G_F \alpha}{2\sqrt{2}\pi} V_{tb} V_{ts}^* \left[C_9^{\text{eff}} \bar{s} \gamma_\mu (1 - \gamma_5) b \bar{l} \gamma_\mu l + C_{10} \bar{s} \gamma_\mu (1 - \gamma_5) b \bar{l} \gamma_\mu \gamma_5 l - 2C_7^{\text{eff}} \frac{m_b}{q^2} \bar{s} i \sigma_{\mu\nu} q^\nu (1 + \gamma_5) b \bar{l} \gamma_\mu l \right],$$

where α is the fine structure constant at Z mass scale, the Cabibbo-Kobayashi-Maskawa matrix elements $|V_{tb} V_{ts}^*| = 0.041$ [63], and the Wilson coefficients $C_7^{\text{eff}} = -0.313$ and $C_{10} = -4.669$ [59]. The effective Wilson coefficient C_9^{eff} includes both the short-distance and long-distance effects as

$$C_9^{\text{eff}} = C_9 + Y_S(q^2) + Y_L(q^2), \quad (25)$$

where $Y_S(q^2)$ describes the short-distance contributions from four-quark operators far away from the resonance regions, which can be calculated reliably in perturbative theory as [60]

$$Y_S(q^2) = 0.124\omega(s) + h(\hat{m}_c, s)C_0 - \frac{1}{2}h(1, s)(4C_3 + 4C_4 + 3C_5 + C_6) - \frac{1}{2}h(0, s)(C_3 + 3C_4) + \frac{2}{9}(3C_3 + C_4 + 3C_5 + C_6), \quad (26)$$

where $s = q^2/m_b^2$, $\hat{m}_c = m_c/m_b$, $C_0 = 3C_1 + C_2 + 3C_3 + C_4 + 3C_5 + C_6$, and

$$\omega(s) = -\frac{2}{9}\pi^2 - \frac{4}{3}\text{Li}_2(s) - \frac{2}{3}\ln(s)\ln(1-s) - \frac{5+4s}{3(1+2s)}\ln(1-s) - \frac{2s(1+s)(1-2s)}{3(1-s)^2(1+2s)}\ln(s) + \frac{5+9s-6s^2}{6(1-s)(1+2s)}. \quad (27)$$

The functional form of the $h(\hat{m}_c, s)$ and $h(0, s)$ are as

$$h(\hat{m}_c, s) = -\frac{8}{9}\ln\frac{m_b}{\mu} - \frac{8}{9}\ln\hat{m}_c + \frac{8}{27} + \frac{4}{9}x - \frac{2}{9}(2+x)|1-x|^{1/2} \begin{cases} \left(\ln \left| \frac{\sqrt{1-x}+1}{\sqrt{1-x}-1} \right| - i\pi \right), & \text{for } x \equiv \frac{4\hat{m}_c^2}{s} < 1 \\ 2 \arctan \frac{1}{\sqrt{x-1}}, & \text{for } x \equiv \frac{4\hat{m}_c^2}{s} > 1 \end{cases} \quad (28)$$

and

$$h(0, s) = \frac{8}{27} - \frac{8}{9}\ln\frac{m_b}{\mu} - \frac{4}{9}\ln s + \frac{4}{9}i\pi. \quad (29)$$

The long-distance contributions, $Y_L(q^2)$ from four-quark operators near the $c\bar{c}$ resonances, cannot be calculated from the first principles of QCD and are usually parametrized in the form of a phenomenological Breit-Wigner formula as [60]

$$Y_L(q^2) = \frac{3\pi}{\alpha^2} \sum_{V_i=J/\psi, \psi(2S)} \frac{\Gamma(V_i \rightarrow l^+l^-) m_{V_i}}{m_{V_i}^2 - q^2 - im_{V_i}\Gamma_{V_i}}. \quad (30)$$

In the range of $4m_l^2 \leq q^2 \leq (m_{B_{(s)}} - m_S)^2$, there are two charm-resonances $J/\psi(3.097)$ and $\psi(3.686)$. To avoid the background of charmonium resonances, it is common to delete the experimental measurements around the resonance regions. For this reason, the long-distance contributions are ignored in our calculations.

Using the parametrization of the aforementioned decays in terms of the form factors, the differential decay width in the rest frame of $B_{(s)}$ -meson can be written as

$$\begin{aligned} \frac{d\Gamma}{dq^2}(B_{(s)} \rightarrow S\nu\bar{\nu}) &= \frac{G_F^2 |V_{tb} V_{ts}^*|^2 m_{B_{(s)}}^3 \alpha^2}{2^8 \pi^5} \frac{|D_\nu(x_t)|^2}{\sin^4 \theta_W} \phi^{3/2}(1, \hat{r}, \hat{s}) |f_+(q^2)|^2, \\ \frac{d\Gamma}{dq^2}(B_{(s)} \rightarrow Sl^+l^-) &= \frac{G_F^2 |V_{tb} V_{ts}^*|^2 m_{B_{(s)}}^3 \alpha^2}{3 \times 2^9 \pi^5} v \phi^{1/2}(1, \hat{r}, \hat{s}) \left[\left(1 + \frac{2\hat{l}}{\hat{s}}\right) \phi(1, \hat{r}, \hat{s}) \alpha_1 + 12\hat{l}\beta_1 \right], \end{aligned} \quad (31)$$

where $\hat{r} = \frac{m_s^2}{m_{B_{(s)}}^2}$, $\hat{s} = \frac{q^2}{m_{B_{(s)}}^2}$, $\hat{l} = \frac{m_l^2}{m_{B_{(s)}}^2}$, $x_t = \frac{m_t^2}{m_W^2}$, $\hat{m}_b = \frac{m_b}{m_{B_{(s)}}}$, $v = \sqrt{1 - \frac{4\hat{l}}{\hat{s}}}$, $\phi(1, \hat{r}, \hat{s}) = 1 + \hat{r}^2 + \hat{s}^2 - 2\hat{r} - 2\hat{s} - 2\hat{r}\hat{s}$, and the functions $D_\nu(x_t)$, α_1 and β_1 are defined as

$$\begin{aligned} D_\nu(x_t) &= \frac{x_t}{8} \left(\frac{2+x_t}{x_t-1} + \frac{3x_t-6}{(x_t-1)^2} \ln x_t \right), \\ \alpha_1 &= \left| C_9^{\text{eff}} f_+(q^2) + \frac{2\hat{m}_b C_7^{\text{eff}} f_T(q^2)}{1 + \sqrt{\hat{r}}} \right|^2 + |C_{10} f_+(q^2)|^2, \\ \beta_1 &= |C_{10}|^2 \left[\left(1 + \hat{r} - \frac{\hat{s}}{2}\right) |f_+(q^2)|^2 + (1 - \hat{r}) \text{Re}[f_+(q^2) f_-^*(q^2)] + \frac{1}{2} \hat{s} |f_-(q^2)|^2 \right]. \end{aligned} \quad (32)$$

The dependency of the differential branching ratios for $B_{(s)} \rightarrow (K_0^*, f_0) l^+ l^- / \nu\bar{\nu}$ on q^2 for both the Exp and LD models as well as the two different fit functions is shown in Figs. 10 and 11.

Integrating Eq. (31) over q^2 in the physical region $4m_l^2 \leq q^2 \leq (m_{B_{(s)}} - m_s)^2$, and using $\tau_{B_{(s)}}$, the branching ratio results of the $B_{(s)} \rightarrow Sl^+l^-/\nu\bar{\nu}$ are obtained. Table VIII shows the branching ratios of the aforementioned decays

for both the Exp and LD models as well as the two different fit functions, in addition to predictions by the conventional LCSR(S2) [21], pQCD(S2) [14], and LFQM(S2) [19].

The polarization asymmetries provide valuable information on the flavor changing loop effects in the SM. The longitudinal lepton polarization asymmetry formula for $B_{(s)} \rightarrow Sl^+l^-$ is given as

$$P_L = \frac{2v}{\left(1 + \frac{2\hat{l}}{\hat{s}}\right) \phi(1, \hat{r}, \hat{s}) \alpha_1 + 12\hat{l}\beta_1} \text{Re} \left[\phi(1, \hat{r}, \hat{s}) \left(C_9^{\text{eff}} f_+(q^2) - \frac{2C_7 f_T(q^2)}{1 + \sqrt{\hat{r}}} \right) (C_{10} f_+(q^2))^* \right], \quad (33)$$

where $v, \hat{l}, \hat{r}, \hat{s}, \phi(1, \hat{r}, \hat{s}), \alpha_1$ and β_1 were defined before. The dependence of the longitudinal lepton polarization asymmetries for the $B_{(s)} \rightarrow (K_0^*, f_0) l^+ l^-$ ($l = \mu, \tau$) decays on the transferred momentum square q^2 for both the Exp and LD models as well as the two different fit functions is plotted in Fig. 12.

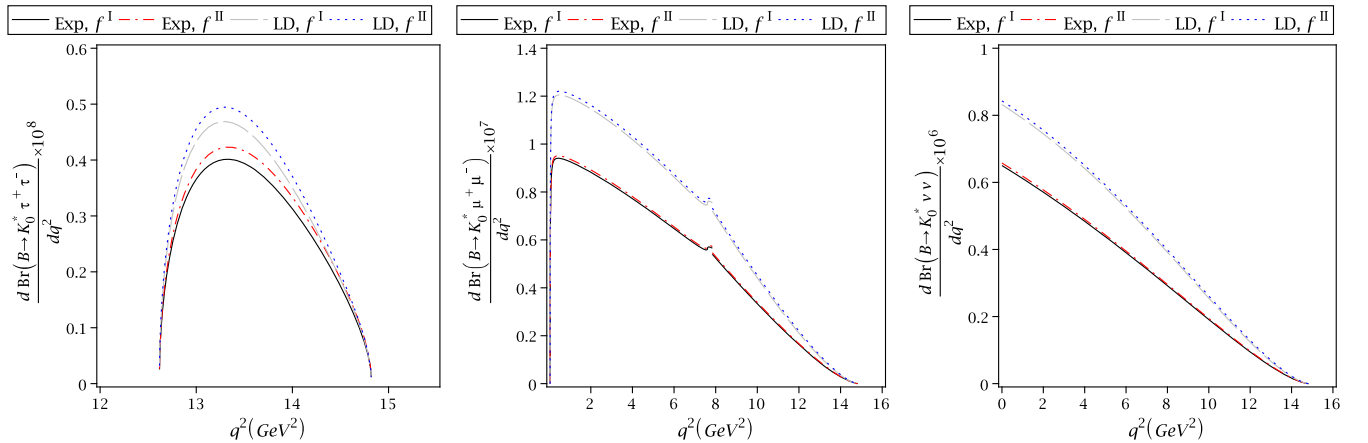
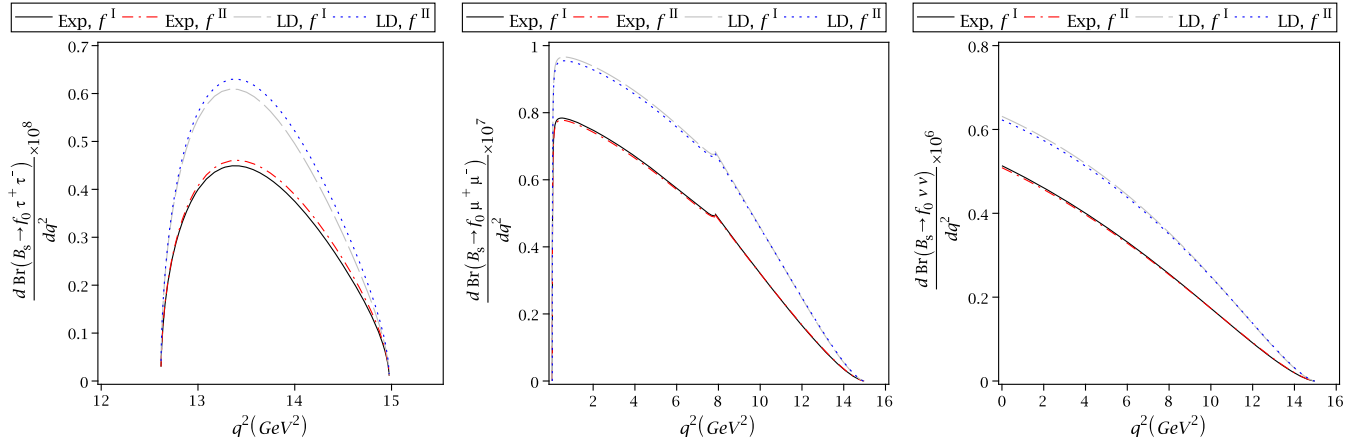


FIG. 10. The differential branching ratios of the semileptonic $B \rightarrow K_0^* l^+ l^- / \nu\bar{\nu}$ decays ($l = \mu, \tau$) on q^2 for both the Exp and LD models as well as the two different fit functions.

FIG. 11. The same as Fig. 10 but for $B_s \rightarrow f_0 l^+ l^- / \nu \bar{\nu}$ decays ($l = \mu, \tau$).

It should be noted that the forward-backward asymmetry for the decay modes $B_{(s)} \rightarrow (K_0^*, f_0) l^+ l^-$ is exactly equal to zero in the SM [64,65], due to the absence of scalar-type coupling between the lepton pair.

In summary, our main goal was to calculate the form factors of the semileptonic decays $B_{(s)} \rightarrow S$ ($S = K_0^*(1430), a_0(1450), f_0(1500)$) in the frame work of the LCSR with the B -meson DAs.

- (i) Two different phenomenological models including exponential and local duality models were used for the shapes of the B -meson DAs.
- (ii) The B -meson DAs were also applied for B_s meson in the $SU(3)_F$ symmetry limit.
- (iii) The form factors of the aforementioned decays were estimated at $q^2 = 0$ through the two exponential and local duality models, and compared with the predictions of other approaches.
- (iv) It was shown that the two-particle leading-twist DA of the B meson φ_+ has the most important contribution in the calculation of the form factors.
- (v) In addition, it was shown that the main sources of the uncertainties in the estimation of the form factors were the shape parameter ω_0 and the decay constants of the scalar mesons.

- (vi) Considering the uncertainties, there was a good agreement between our results in the exponential model and predictions of the conventional LCSR in scenario 2. As a result, our calculations confirmed that the scalar mesons $K_0^*(1430), a_0(1450)$, and $f_0(1500)$ can be viewed as the lowest lying states with two quarks in the quark model.
- (vii) For a better analysis, the results obtained for the form factors via the B -meson LCSR method were parametrized to the two different fit functions. The form factors obtained by both fit functions were very consistent in each case.
- (viii) Using the form factors $f_+(q^2), f_-(q^2)$, and $f_T(q^2)$, the branching ratio values for the semileptonic $B_s \rightarrow K_0^* l \bar{\nu}_l$ and $B \rightarrow a_0 l \bar{\nu}_l$ decays, and also the FCNC semileptonic transitions $B \rightarrow K_0^*$ and $B_s \rightarrow f_0$ were calculated.
- (ix) The dependence of the differential branching ratios as well as the longitudinal lepton polarization asymmetries for the aforementioned decays were plotted with respect to q^2 .
- (x) Future experimental measurements can give valuable information about these aforesaid decays and the nature of the scalar mesons.

TABLE VIII. The branching ratio values of $B_{(s)} \rightarrow (K_0^*, f_0) l^+ l^- / \nu \bar{\nu}$ for both the Exp and LD models as well as the two different fit functions in addition to the LCSR, pQCD, and LFQM approaches.

Mode	This work				LCSR(S2) [21]	pQCD(S2) [14]	LFQM(S2) [19]
	Exp, f^I	Exp, f^{II}	LD, f^I	LD, f^{II}			
$\text{Br}(B \rightarrow K_0^* \nu \bar{\nu}) \times 10^6$	$4.40_{-0.90}^{+1.35}$	$4.78_{-0.95}^{+1.43}$	$6.22_{-1.24}^{+1.87}$	$6.32_{-1.26}^{+1.90}$
$\text{Br}(B \rightarrow K_0^* \mu^+ \mu^-) \times 10^7$	$5.66_{-1.98}^{+2.77}$	$6.03_{-2.11}^{+2.95}$	$7.89_{-2.76}^{+3.86}$	$8.03_{-2.81}^{+3.93}$	$5.6_{-2.3}^{+3.1}$	$9.78_{-4.40}^{+7.66}$	1.62
$\text{Br}(B \rightarrow K_0^* \tau^+ \tau^-) \times 10^8$	$0.55_{-0.28}^{+0.36}$	$0.61_{-0.31}^{+0.40}$	$0.65_{-0.33}^{+0.42}$	$0.69_{-0.35}^{+0.44}$	$0.98_{-0.55}^{+1.24}$	$0.63_{-0.30}^{+0.57}$	0.29
$\text{Br}(B_s \rightarrow f_0 \nu \bar{\nu}) \times 10^6$	$3.97_{-0.71}^{+1.07}$	$4.14_{-0.75}^{+1.12}$	$5.52_{-0.99}^{+1.49}$	$5.46_{-0.98}^{+1.47}$
$\text{Br}(B_s \rightarrow f_0 \mu^+ \mu^-) \times 10^7$	$5.00_{-1.35}^{+1.95}$	$5.22_{-1.41}^{+2.04}$	$7.00_{-1.89}^{+2.73}$	$6.92_{-1.87}^{+2.70}$	$5.2_{-1.7}^{+2.3}$	$10.0_{-3.8}^{+8.5}$...
$\text{Br}(B_s \rightarrow f_0 \tau^+ \tau^-) \times 10^8$	$0.65_{-0.21}^{+0.38}$	$0.71_{-0.23}^{+0.41}$	$0.90_{-0.30}^{+0.53}$	$0.95_{-0.31}^{+0.56}$	$1.2_{-0.5}^{+0.8}$	$1.3_{-0.6}^{+1.2}$...

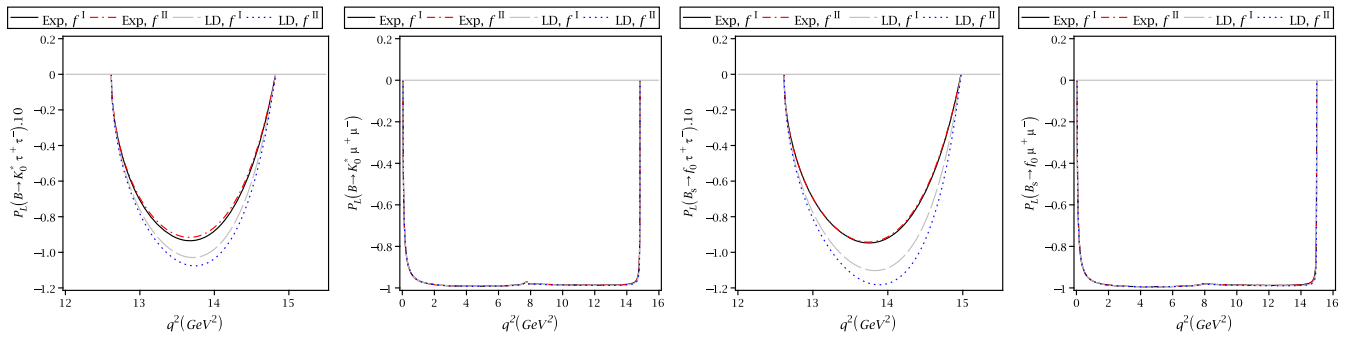


FIG. 12. The dependence of the longitudinal lepton polarization asymmetries on q^2 for both the Exp and LD models as well as the two different fit functions.

- [1] R. L. Jaffe, *Phys. Rev. D* **15**, 267 (1977).
- [2] U. G. Meissner, *Comments Nucl. Part. Phys.* **20**, 119 (1991).
- [3] D. Horn and J. Mandula, *Phys. Rev. D* **17**, 898 (1978).
- [4] H. Fritzsch and M. Gell-Mann, *eConf C720906V2*, 135 (1972).
- [5] M. Piotrowska, [arXiv:2105.08557](https://arxiv.org/abs/2105.08557).
- [6] E. Klempt, *Phys. Lett. B* **820**, 136512 (2021).
- [7] H. Y. Cheng, C. K. Chua, and K. C. Yang, *Phys. Rev. D* **73**, 014017 (2006).
- [8] M. Ablikim *et al.* (BESIII Collaboration), *Phys. Rev. D* **104**, 071101 (2021).
- [9] M. Ablikim *et al.* (BESIII Collaboration), *Phys. Rev. D* **105**, L051103 (2022).
- [10] M. Ablikim *et al.* (BESIII Collaboration), [arXiv:2303.12927](https://arxiv.org/abs/2303.12927).
- [11] T. Abe *et al.* (Belle Collaboration), *Phys. Rev. Lett.* **96**, 251803 (2006); P. Chang *et al.* (Belle Collaboration), *Phys. Lett. B* **599**, 148 (2004); M. Prim *et al.* (Belle Collaboration), *Phys. Rev. D* **88**, 072004 (2013); M. Prim *et al.* (Belle Collaboration), *Phys. Rev. D* **81**, 071101 (2010).
- [12] J. P. Lees *et al.* (BABAR Collaboration), *Phys. Rev. D* **85**, 112010 (2012); **83**, 112010 (2011); B. Aubert *et al.* (BABAR Collaboration), *Phys. Rev. D* **79**, 052005 (2009); **78**, 012004 (2008); *Phys. Rev. Lett.* **101**, 161801 (2008); *Phys. Rev. D* **78**, 092008 (2008); J. P. Lee *et al.* (BABAR Collaboration), *Phys. Rev. D* **85**, 072005 (2012); B. Aubert *et al.* (BABAR Collaboration), *Phys. Rev. D* **76**, 071103 (2007); J. P. Lees *et al.* (BABAR Collaboration), *Phys. Rev. D* **83**, 112010 (2011).
- [13] R. Aaij *et al.* (LHCb Collaboration), *J. High Energy Phys.* **06** (2019) 114; **07** (2019) 032.
- [14] R. H. Li, C. D. Lü, W. Wang, and X. X. Wang, *Phys. Rev. D* **79**, 014013 (2009).
- [15] H. Y. Cheng, C. K. Chua, and C. W. Hwang, *Phys. Rev. D* **69**, 074025 (2004).
- [16] T. M. Aliev, K. Azizi, and M. Savci, *Phys. Rev. D* **76**, 074017 (2007).
- [17] M. Z. Yang, *Phys. Rev. D* **73**, 034027 (2006).
- [18] N. Ghahramany and R. Khosravi, *Phys. Rev. D* **80**, 016009 (2009).
- [19] C. H. Chen, C. Q. Geng, C. C. Lih, and C. C. Liu, *Phys. Rev. D* **75**, 074010 (2007).
- [20] M. J. Aslam, C. D. Lü, and Y. M. Wang, *Phys. Rev. D* **79**, 074007 (2009).
- [21] Y. M. Wang, M. J. Aslam, and C. D. Lü, *Phys. Rev. D* **78**, 014006 (2008).
- [22] Z. G. Wang, *Eur. Phys. J. C* **75**, 50 (2015).
- [23] Z. G. Wang, *Nucl. Phys.* **B898**, 431 (2015).
- [24] Y. J. Sun, Z. H. Li, and T. Huang, *Phys. Rev. D* **83**, 025024 (2011).
- [25] D. Huang, T. Zhong, H. B. Fu, Z. H. Wu, X. G. Wu, and H. Tong, *Eur. Phys. J. C* **83**, 680 (2023).
- [26] H. Y. Han, X. G. Wu, H. B. Fu, Q. L. Zhang, and T. Zhong, *Eur. Phys. J. C* **49**, 78 (2013).
- [27] A. Khodjamirian, T. Mannel, and N. Offen, *Phys. Lett. B* **620**, 52 (2005).
- [28] F. De Fazio, T. Feldmann, and T. Hurth, *Nucl. Phys.* **B733**, 1 (2006).
- [29] X. Y. Han, L. S. Lu, C. D. Lü, Y. L. Shen, and B. X. Shi, *J. High Energy Phys.* **11** (2023) 091.
- [30] R. Khosravi, *Phys. Rev. D* **105**, 116027 (2022).
- [31] V. M. Braun, Y. Ji, and A. N. Manashov, *J. High Energy Phys.* **05** (2017) 022.
- [32] C. D. Lü, Y. L. Shen, Y. M. Wang, and Y. B. Wei, *J. High Energy Phys.* **01** (2019) 024.
- [33] A. Khodjamirian, T. Mannel, and N. Offen, *Phys. Rev. D* **75**, 054013 (2007).
- [34] I. I. Balitsky and V. M. Braun, *Nucl. Phys.* **B311**, 541 (1989).
- [35] N. Gubernari, A. Kokulu, and D. van Dyk, *J. High Energy Phys.* **01** (2019) 150.
- [36] P. A. Zyla *et al.* (Particle Data Group), *Prog. Theor. Exp. Phys.* **2020**, 083C01 (2020).
- [37] S. Aoki, Y. Aoki, D. Becirevic *et al.* (FLAG Review 2019 Collaboration), *Eur. Phys. J. C* **80**, 113 (2020).

- [38] Y. M. Wang and Y. L. Shen, *Nucl. Phys.* **B898**, 563 (2015).
- [39] V. M. Braun and A. Khodjamirian, *Phys. Lett. B* **718**, 1014 (2013).
- [40] Y. M. Wang, Y. B. Wei, Y. L. Shen, and C. D. Lü, *J. High Energy Phys.* **06** (2017) 062.
- [41] V. M. Braun, A. N. Manashov, and N. Offen, *Phys. Rev. D* **92**, 074044 (2015).
- [42] M. Rahimi and M. Wald, *Phys. Rev. D* **104**, 016027 (2021).
- [43] B. O. Lange and M. Neubert, *Phys. Rev. Lett.* **91**, 102001 (2003).
- [44] M. Beneke, G. Buchalla, M. Neubert, and C. T. Sachrajda, *Nucl. Phys.* **B591**, 313 (2000).
- [45] A. Heller *et al.* (Belle Collaboration), *Phys. Rev. D* **91**, 112009 (2015).
- [46] T. Janowski, B. Pullin, and R. Zwicky, *J. High Energy Phys.* **12** (2021) 008.
- [47] A. Khodjamirian, R. Mandal, and T. Mannel, *J. High Energy Phys.* **10** (2020) 043.
- [48] V. M. Braun, Y. Ji, and A. N. Manashov, *Phys. Rev. D* **100**, 014023 (2019); W. Wang, Y. M. Wang, J. Xu, and S. Zhao, *Phys. Rev. D* **102**, 011502 (2020); S. Zhao and A. V. Radyushkin, *Phys. Rev. D* **103**, 054022 (2021).
- [49] A. G. Grozin and M. Neubert, *Phys. Rev. D* **55**, 272 (1997).
- [50] S. D. Genon and C. T. Sachrajda, *Nucl. Phys.* **B650**, 356 (2003).
- [51] V. M. Braun, D. Yu. Ivanov, and G. P. Korchemsky, *Phys. Rev. D* **69**, 034014 (2004).
- [52] S. J. Lee and M. Neubert, *Phys. Rev. D* **72**, 094028 (2005).
- [53] F. D. Fazio, T. Feldmann, and T. Hurth, *J. High Energy Phys.* **02** (2008) 031.
- [54] M. Beneke, V. Braun, Y. Ji, and Y. B. Wei, *J. High Energy Phys.* **07** (2018) 154.
- [55] A. M. Galda and M. Neubert, *Phys. Rev. D* **102**, 071501 (2020).
- [56] D. S. Du, J. W. Li, and M. Z. Yang, *Phys. Lett. B* **619**, 105 (2005).
- [57] P. Colangelo, F. D. Fazio, and W. Wang, *Phys. Rev. D* **81**, 074001 (2010).
- [58] Y. J. Sun, Z. H. Li, and T. Huang, *Phys. Rev. D* **83**, 025024 (2011).
- [59] B. Grinstein, M. J. Savage, and M. B. Wise, *Nucl. Phys.* **B319**, 271 (1989); M. Misiak, *Nucl. Phys.* **B393**, 23 (1993).
- [60] A. J. Buras and M. Munz, *Phys. Rev. D* **52**, 186 (1995); G. Buchalla, A. J. Buras, and M. E. Lautenbacher, *Rev. Mod. Phys.* **68**, 1125 (1996).
- [61] A. Khodjamirian, T. Mannel, and Y. M. Wang, *J. High Energy Phys.* **02** (2013) 010.
- [62] A. Khodjamirian and A. V. Rusov, *J. High Energy Phys.* **08** (2017) 112.
- [63] D. King, M. Kirk, A. Lenz, and T. Rauh, *J. High Energy Phys.* **03** (2020) 112.
- [64] G. Belanger, C. Q. Geng, and P. Turcotte, *Nucl. Phys.* **B390**, 253 (1993).
- [65] C. Q. Geng and C. P. Kao, *Phys. Rev. D* **54**, 5636 (1996).